Physics Letters B 753 (2016) 41–56

Contents lists available at ScienceDirect

Physics Letters B

www.elsevier.com/locate/physletb

Elliptic flow of muons from heavy-flavour hadron decays at forward rapidity in Pb–Pb collisions at $\sqrt{s_{NN}} = 2.76$ TeV

ALICE Collaboration *

ARTICLE INFO

Article history:
Received 15 July 2015
Received in revised form 19 November 2015
Accepted 20 November 2015
Available online 2 December 2015
Editor: L. Rolandi

Keywords:
LHC
ALICE experiment
Pb–Pb collisions
Heavy-flavour decay muons
Elliptic flow

ABSTRACT

The elliptic flow, v_2, of muons from heavy-flavour hadron decays at forward rapidity ($2.5 < y < 4$) is measured in Pb–Pb collisions at $\sqrt{s_{NN}} = 2.76$ TeV with the ALICE detector at the LHC. The scalar product, two- and four-particle Q cumulants and Lee–Yang zeros methods are used. The dependence of the v_2 of muons from heavy-flavour hadron decays on the collision centrality, in the range 0–40%, and on transverse momentum, p_T, is studied in the interval $3 < p_T < 10$ GeV/c. A positive v_2 is observed with the scalar product and two-particle Q cumulants in semi-central collisions (10–20% and 20–40% centrality classes) for the p_T interval from 3 to about 5 GeV/c with a significance larger than 3σ, based on the combination of statistical and systematic uncertainties. The v_2 magnitude tends to decrease towards more central collisions and with increasing p_T. It becomes compatible with zero in the interval $6 < p_T < 10$ GeV/c. The results are compared to models describing the interaction of heavy quarks and open heavy-flavour hadrons with the high-density medium formed in high-energy heavy-ion collisions.

1. Introduction

Experiments with ultra-relativistic heavy-ion collisions aim at investigating the properties of strongly-interacting matter at very high temperatures and energy densities. Quantum Chromodynamics (QCD) calculations on the lattice predict, under these conditions, the formation of a Quark–Gluon Plasma (QGP), where color confinement vanishes and chiral symmetry is partially restored [1–5]. Heavy quarks (charm and beauty) are created in initial hard-scattering processes on a time scale shorter than the QGP formation time. Subsequently, they interact with the medium constituents via inelastic [6,7] and elastic [8–10] processes. Therefore, heavy quarks are regarded as effective probes of the QGP properties.

Heavy-quark energy loss due to in-medium interactions can be studied by means of the nuclear modification factor R_{AA}, defined as the ratio of the yield of heavy-flavour particles measured in nucleus–nucleus (AA) collisions to that observed in proton–proton (pp) collisions scaled by the number of binary nucleon–nucleon collisions. The PHENIX and STAR Collaborations measured, in central Au–Au collisions at $\sqrt{s_{NN}} = 200$ GeV, a strong suppression corresponding to a R_{AA} of about 0.2–0.3 for heavy-flavour decay electrons at mid-rapidity (y) and transverse momentum $p_T > 5$ GeV/c [11–17]. A similar suppression was also measured by the STAR Collaboration for mid-rapidity D^0 mesons [18]. A significant suppression was also observed by the PHENIX Collaboration at forward rapidity for muons from heavy-flavour hadron decays in central Cu–Cu collisions at $\sqrt{s_{NN}} = 200$ GeV [19]. At the LHC, the ALICE Collaboration reported a similar effect in central Pb–Pb collisions at $\sqrt{s_{NN}} = 2.76$ TeV for D mesons at mid-rapidity [20] and muons from heavy-flavour hadron decays at forward rapidity [21] in the interval $2 < p_T < 16$ GeV/c and $4 < p_T < 10$ GeV/c, respectively. The CMS Collaboration measured a significant suppression of non-prompt J/ψ from beauty-hadron decays in the interval $6.5 < p_T < 30$ GeV/c ($3 < p_T < 30$ GeV/c) and $|y| < 2.4$ ($1.6 < |y| < 2.4$) [22,23]. A first measurement of non-prompt J/ψ by the ALICE Collaboration at mid-rapidity ($|y| < 0.8$) and in the interval $4.5 < p_T < 10$ GeV/c has been recently published [24].

Further insights into the QGP evolution and the in-medium interactions can be gained from the study of the azimuthal anisotropy of particles carrying heavy quarks which, in contrast to light quarks, have experienced the full system evolution. The study of azimuthal anisotropy is a field of intense experimental and theoretical investigations (see [25] and references therein). In non-central collisions, the initial spatial anisotropy of the overlap region, elongated in the direction perpendicular to the reaction plane, defined by the beam axis and the impact parameter of the collision, is converted into an anisotropy in momentum space through rescatterings [26]. Experimentally, the study of the particle azimuthal anisotropy is based on a Fourier expansion of azimuthal distributions given by:

* *E-mail address:* alice-publications@cern.ch.

http://dx.doi.org/10.1016/j.physletb.2015.11.059
0370-2693/

$$\frac{\mathrm{d}^2N}{\mathrm{d}p_\mathrm{T}\mathrm{d}\varphi} = \frac{1}{2\pi}\frac{\mathrm{d}N}{\mathrm{d}p_\mathrm{T}}\left(1+2\sum_{n=1}^{\infty} v_n(p_\mathrm{T})\cos[n(\varphi-\Psi_n)]\right), \quad (1)$$

where φ and p_T are the particle azimuthal angle and transverse momentum, respectively. The Fourier coefficients, v_n, characterize the anisotropy of produced particles and Ψ_n is the azimuthal angle of the initial-state symmetry plane for the nth harmonic, introduced to account for the event-by-event fluctuations of the initial nucleon density profile. The second Fourier coefficient, v_2, which can also be expressed as $v_2 = \langle\cos[2(\varphi-\Psi_2)]\rangle$, is named elliptic flow.

The v_2 of heavy-flavour hadrons is expected to provide information on the collective expansion and degree of thermalization of heavy quarks in the medium at low p_T ($p_\mathrm{T} < 2$–3 GeV/c). The participation of heavy quarks in the collective expansion is expected to give a positive v_2 [26]. Moving towards intermediate p_T ($3 < p_\mathrm{T} < 6$ GeV/c), the v_2 Fourier coefficient is also expected to be sensitive to the presence of recombination processes in the hadronization of heavy quarks [27,28]. At high p_T ($p_\mathrm{T} > 6$ GeV/c), the v_2 measurement can constrain the path-length dependence of the in-medium parton energy loss, which becomes the dominant contribution to the azimuthal anisotropy and is also predicted to give a positive v_2 [29,30], thus complementing the R_AA measurement.

The PHENIX Collaboration reported a positive v_2 of heavy-flavour decay electrons at mid-rapidity in Au–Au collisions at $\sqrt{s_\mathrm{NN}} = 200$ GeV, reaching a maximum value of about 0.15 at $p_\mathrm{T} = 1.5$ GeV/c in semi-central collisions [14,15,31]. A similar behavior was also observed by the STAR Collaboration [32]. Recently, a v_2 value significantly larger than zero was measured for D mesons at mid-rapidity in Pb–Pb collisions at $\sqrt{s_\mathrm{NN}} = 2.76$ TeV [33,34]. A complementary measurement at the same energy, provided by the heavy-flavour decay muon elliptic flow at forward rapidity ($2.5 < y < 4$), is of great interest in order to provide new constraints for models that implement the heavy-quark interactions with the medium. Finally, the measurement is also important for the interpretation of the J/ψ elliptic flow results at forward rapidity [35] in terms of a regeneration production from deconfined charm quarks in the medium.

In this Letter, we present the measurement of the elliptic flow of muons from heavy-flavour hadron decays at forward rapidity ($2.5 < y < 4$) in Pb–Pb collisions at $\sqrt{s_\mathrm{NN}} = 2.76$ TeV recorded with the ALICE detector. The elliptic flow is measured using different methods: scalar product [36], two- and four-particle Q cumulants [37,38] and Lee–Yang zeros [39–41]. These methods exhibit different sensitivities to flow fluctuations and correlations not related to the azimuthal asymmetry in the initial geometry (non-flow effects). The v_2 coefficient is measured as a function of p_T in the interval $3 < p_\mathrm{T} < 10$ GeV/c and in three centrality classes in the range 0–40%. The centrality dependence of v_2 is presented in the interval $3 < p_\mathrm{T} < 5$ GeV/c.

The Letter is organized as follows. The ALICE detector, with an emphasis on the muon spectrometer, and the data sample are presented in Section 2. The analysis details, the methods for the v_2 measurement, the inclusive muon v_2 determination, the procedure for the subtraction of the background of muons from decays of light-flavour hadrons and the study of systematic uncertainties, are described in Section 3. The v_2 results for muons from heavy-flavour decays are presented in Section 4. The v_2 measurement in semi-central collisions as well as the published R_AA in central collisions are compared to model calculations in Section 5. Finally, conclusions are given in Section 6.

2. ALICE experiment and data sample

The ALICE detector is described in detail in [42,43]. The apparatus is composed of a set of central barrel detectors (pseudo-rapidity coverage $|\eta| < 0.9$) located inside a solenoid magnet that generates a field of 0.5 T parallel to the beam direction, a muon spectrometer ($-4 < \eta < -2.5$[1]) and a set of detectors for event characterization and triggering located in the forward and backward η regions. The muon spectrometer consists of a passive front absorber made of carbon, concrete and steel, a beam shield, a 3 T m dipole magnet, tracking chambers, a muon filter (iron wall) and trigger chambers. The muon tracking system is composed of five stations, each including two planes of cathod pad chambers, with the third station inside the dipole magnet. The muon tracking system is completed by four trigger planes of resistive plate chambers downstream of the iron wall, which absorbs hadrons that punch through the front absorber, as well as secondary particles produced inside it and low momentum muons ($p < 4$ GeV/c).

Two scintillator arrays (V0) covering the pseudo-rapidity intervals $-3.7 < \eta < -1.7$ and $2.8 < \eta < 5.1$ are used for triggering, for collision centrality determination and for beam-induced background rejection. The Zero Degree Calorimeters (ZDC), located at 114 m from the centre of the detector on both sides, can detect spectator protons and neutrons and are also used for the offline rejection of beam-induced background and electromagnetic interactions. The Silicon Pixel Detector (SPD), that composes the two innermost layers of the Inner Tracking System (ITS), is used for the interaction vertex reconstruction. The Time Projection Chamber (TPC), which measures charged-particle tracks with full azimuthal coverage in $|\eta| < 0.9$, is used in this analysis for the measurement of the reference particles (Section 3.1).

The results presented in this Letter are obtained from the data sample recorded with ALICE during the 2011 Pb–Pb run. The data were collected with a minimum-bias trigger requiring the coincidence of signals in the two V0 arrays in synchronization with the passage of two crossing bunches. In addition, the recorded event sample was enriched with central and semi-central Pb–Pb collisions by applying thresholds, at the trigger level, on the V0 signal amplitude. The beam-induced background (beam–gas interactions) was reduced by using the timing information from the V0 and ZDC detectors. Furthermore, a minimal energy deposit in the ZDC was required to reject the contribution from electromagnetic Pb–Pb interactions. Only events with a reconstructed primary vertex within ± 10 cm from the nominal position of the interaction vertex along the beam direction are analyzed. The Pb–Pb collisions are classified according to their degree of centrality by means of the sum of the amplitudes of the signals in the V0 detector and the centrality classes are defined as percentiles of the total hadronic Pb–Pb cross section [44]. The analysis is carried out in three centrality classes: 0–10% (using the sample with trigger on central collisions), 10–20% and 20–40% (using the sample with trigger on semi-central collisions). The analyzed data sample corresponds to an integrated luminosity of 11.3 μb^{-1} in the 0–10% centrality class and of 3.5 μb^{-1} in the other two centrality classes.

3. Data analysis

The elliptic flow of muons from heavy-flavour hadron decays, $v_2^{\mu\leftarrow\mathrm{HF}}$, is obtained from the measurement of the inclusive muon elliptic flow, v_2^{μ}, by subtracting the elliptic flow of muons from pri-

[1] In the ALICE reference frame, the muon spectrometer covers a negative η range and consequently a negative y range. In the following, given that the colliding system is symmetric, the results are presented with a positive y notation.

mary charged pion and kaon decays $v_2^{\mu\leftarrow\pi,\mathrm{K}}$ (Sections 3.1 and 3.4), as:

$$v_2^{\mu\leftarrow\mathrm{HF}} = \frac{v_2^{\mu} - f^{\mu\leftarrow\pi,\mathrm{K}} \cdot v_2^{\mu\leftarrow\pi,\mathrm{K}}}{1 - f^{\mu\leftarrow\pi,\mathrm{K}}}, \quad (2)$$

where $f^{\mu\leftarrow\pi,\mathrm{K}}$ is the muon background fraction, defined as the ratio of the yield of muons from primary charged pion and kaon decays to that of inclusive muons. The measurement of the $v_2^{\mu\leftarrow\mathrm{HF}}$ coefficient is carried out in the interval $3 < p_{\mathrm{T}} < 10$ GeV/c in order to limit the systematic uncertainty on the subtraction of the muon background contribution.

3.1. Track selection

The selection criteria for particles of interest, muon tracks, are similar to those used in the previous analyses of pp collisions at $\sqrt{s} = 2.76$ TeV and 7 TeV and Pb–Pb collisions at $\sqrt{s_{\mathrm{NN}}} = 2.76$ TeV [21,45]. The tracks are required to be within the geometrical acceptance of the muon spectrometer, with $-4 < \eta < -2.5$ and $170° < \theta_{\mathrm{abs}} < 178°$, where θ_{abs} is the polar angle measured at the end of the absorber. In order to improve the muon identification, a reconstructed track in the tracking chambers is required to match a track segment in the trigger chambers. This leads to a very efficient rejection of the background produced by charged hadrons, which are absorbed in the iron wall. Furthermore, a cut on the product $p \cdot DCA$ of the track momentum p and distance of closest approach (DCA) to the primary vertex is applied to remove the beam-induced background tracks and fake tracks coming from the superposition of several particles crossing the muon spectrometer. Due to multiple scattering in the front absorber, the DCA distribution of tracks coming form the interaction vertex is expected to be described by a Gaussian function, its width being dependent on the absorber material and proportional to $1/p$. Background tracks have a very broad distribution in $p \cdot DCA$ and are effectively rejected by a cut at 6σ, where σ is extracted from a Gaussian fit to the $p \cdot DCA$ distribution measured in two intervals of θ_{abs}, corresponding to different materials in the front absorber. The relative momentum resolution of reconstructed tracks varies from about 1% to 4% for tracks with momentum between 20 GeV/c and 100 GeV/c. After the cuts are applied, in the region $p_{\mathrm{T}} > 3$ GeV/c the residual background to heavy-flavour decay muons consists of muons from decays of primary charged pions and kaons[2] and it amounts to 5–15%, depending on p_{T} and on collision centrality (Section 3.4).

The mid-rapidity charged-particle tracks used to determine the flow vector $\vec{Q}_n$ or the generating function (Section 3.2) are called in the following reference particles. They are defined as tracks measured in the TPC in $|\eta| < 0.8$. These are required to have at least 70 associated space points out of the maximum of 159, a χ^2 per degree of freedom (ndf) for the momentum fit in the range $\chi^2/\mathrm{ndf} < 2$ and a transverse momentum value in the interval $0.2 < p_{\mathrm{T}} < 5$ GeV/c. Additionally, tracks are rejected if their distance of closest approach to the primary vertex is larger than 3 cm in the plane transverse to the beam direction or in the longitudinal direction.

3.2. Flow analysis methods

The elliptic flow measurement is carried out using various methods that have different sensitivities to flow fluctuations and non-flow effects [46]. Flow fluctuations are mainly due to event-by-event fluctuations of the initial density profile, while non-flow effects correspond to correlations not related to the azimuthal anisotropy in the initial state, such as resonance decays, jets and Bose–Einstein correlations between identical particles. It is worth mentioning that, in the present analysis, most of these non-flow effects are strongly suppressed by introducing an η gap between reference particles and particles of interest [47]. In this analysis, the scalar product [36], two- and four-particle Q cumulants [37,38] and Lee–Yang zeros [39–41] methods are employed. The description of these methods will be limited to the features specific to the present analysis. The following notations are introduced: $v_2^{\mu(\mu\leftarrow\mathrm{HF})}\{\mathrm{SP}\}$, refers to the measurement using the scalar product, $v_2^{\mu(\mu\leftarrow\mathrm{HF})}\{2\}$ and $v_2^{\mu(\mu\leftarrow\mathrm{HF})}\{4\}$ correspond to the ones using the two-particle Q cumulants and four-particle Q cumulants, while $v_2^{\mu(\mu\leftarrow\mathrm{HF})}\{\mathrm{LYZ\text{-}Prod}\}$ and $v_2^{\mu(\mu\leftarrow\mathrm{HF})}\{\mathrm{LYZ\text{-}Sum}\}$ are obtained using Lee–Yang zeros with product and sum generating functions. The superscripts μ and $\mu \leftarrow \mathrm{HF}$ refer to inclusive muons and muons from heavy-flavour hadron decays, respectively. It is worth mentioning that these methods are more accurate than the standard event plane method, which yields a measurement lying between the event-averaged mean value and the root-mean-square value in the presence of flow fluctuations [48,49]. Moreover, the multi-particle correlation methods (four-particle Q cumulants and Lee–Yang zeros) are less affected by non-flow correlations than two-particle correlation methods, but they cannot be used reliably when the muon flow magnitude is small and when the number of muons is small in the selected phase-space region e.g. in central and peripheral collisions, respectively [37,39]. Under these conditions, the scalar product and two-particle cumulant methods provide a v_2 measurement in a wider centrality range.

The scalar product method [36,48], derived from the standard event plane technique [48], is based on the measurement of the flow vector $\vec{Q}_n$ [36] computed from reference particles. In order to determine the elliptic flow, the $\vec{Q}_2$ vector in a given event is expressed as:

$$\vec{Q}_2 = \left(\sum_{j=1}^{N} \cos 2\varphi_j, \sum_{j=1}^{N} \sin 2\varphi_j\right), \quad (3)$$

where φ_j is the particle azimuthal angle and N is the multiplicity of reference particles.

With this method the 2nd harmonic coefficient is given by:

$$v_2\{\mathrm{SP}\} = \frac{\langle \vec{Q}_2 \cdot \vec{u}_{2,i}(\eta, p_{\mathrm{T}})\rangle}{2\sqrt{\langle \vec{Q}_2^{\mathrm{A}} \cdot \vec{Q}_2^{\mathrm{B}}\rangle}}, \quad (4)$$

where the brackets in the numerator indicate the average over muons at forward rapidity, in all events. The vector Q_2 is calculated from Eq. (3) and the vector $\vec{u}_{2,i} = (\cos 2\varphi_i, \sin 2\varphi_i)$ is the unit vector of the ith muon. In the denominator, each sample of reference particles used to compute $\vec{Q}_2$ is divided into two sub-samples of same multiplicity in symmetrical η intervals, $-0.8 < \eta < -0.5$ and $0.5 < \eta < 0.8$, separated by a η gap of one unit of pseudo-rapidity, labeled with the superscripts A and B and the brackets correspond to the average over events.

The cumulant technique [37,38] is based on a cumulant expansion of multi-particle azimuthal correlations. Different order cumulants have different sensitivities to flow fluctuations. In the present analysis, two- and four-particle cumulants are used to extract the muon elliptic flow. The results presented in the following are obtained from a direct calculation of multi-particle cumulants performed by using the Q-cumulant technique [38], which is based on the moments of the magnitude of the flow vector $\vec{Q}_2$. It is

[2] Note that the contribution of muons from secondary light hadron decays produced inside the front absorber is negligible for $p_{\mathrm{T}} > 3$ GeV/c [45].

worth mentioning that in this approach the cumulants are not biased by the interferences between various harmonics. The reference elliptic flow values V_2 evaluated from the 2nd order cumulant $c_2\{2\}$ and 4th order cumulant $c_2\{4\}$ with reference particles are given by $V_2\{2\} = \sqrt{c_2\{2\}}$ and $V_2\{4\} = \sqrt[4]{-c_2\{4\}}$, respectively. Once the reference elliptic flow is estimated, the muon elliptic flow with respect to the reference elliptic flow is obtained from the 2nd and 4th order cumulants according to:

$$v_2\{2\} = \frac{d_2\{2\}}{V_2\{2\}} \text{ and } v_2\{4\} = \frac{d_2\{4\}}{V_2\{4\}^3}, \tag{5}$$

where $d_2\{2\}$ and $d_2\{4\}$ are the 2nd and 4th order cumulants of selected muons [38].

The Lee–Yang zeros method [39–41] relies on correlations involving all particles in the event. This is the limit of cumulants when the order of cumulants goes to infinity. The method is based on the location of the zeros in the complex plane, of a generating function of azimuthal correlations, which relates the position of the first minimum of the generating function to the magnitude of the reference elliptic flow V_2 defined as:

$$V_2 \equiv \left\langle \sum_{j=1}^{M} \cos[2(\varphi_j - \Psi_2)] \right\rangle_{\text{events}}, \tag{6}$$

where M is the multiplicity of reference particles and the average is taken over all events. For this purpose, the following complex-valued generating function is evaluated as a function of a positive real variable r and few, typically five, equally spaced reference angles ϑ (LYZ-Prod method):

$$G^{\vartheta}(ir) \equiv \left\langle \prod_{j=1}^{M} (1 + ir\cos[2(\varphi_j - \vartheta)]) \right\rangle_{\text{events}}. \tag{7}$$

The first positive minimum of $|G^{\vartheta}(ir)|$, denoted as r_0^{ϑ}, allows one to estimate V_2^{ϑ}, which can be written as $V_2^{\vartheta} = j_{01}/r_0^{\vartheta}$, where $j_{01} \simeq 2.405$ is the first root of the Bessel function. Once the first minimum r_0^{ϑ} is determined, the differential muon elliptic flow is estimated with respect to the reference flow V_2^{ϑ} as detailed in [41]. Finally, the result is averaged over all ϑ angles. An alternative form of the generating function provided with the LYZ-Sum method is:

$$G^{\vartheta}(ir) \equiv \left\langle \exp\left(ir \sum_{j=1}^{M} \cos[2(\varphi_j - \vartheta)] \right) \right\rangle_{\text{events}}. \tag{8}$$

The version of the method involving a product for the construction of the generation function (Eq. (7)) was designed to disentangle interferences between different harmonics, which is not the case with the generating function using a sum of the individual reference particle contributions. Both generating functions are used in this analysis.

Note that, for all methods, autocorrelation effects are avoided because the particles (muons) used in the determination of the flow are not included in the estimation of the reference flow.

3.3. Inclusive muon elliptic flow

The elliptic flow of inclusive muons, v_2^{μ}, is studied with two-particle correlation methods (scalar product and two-particle Q cumulants) in the centrality intervals 0–10%, 10–20% and 20–40%. In the 20–40% centrality interval, the multi-particle correlation methods (four-particle Q cumulants and Lee–Yang zeros) are also used.

Several sources of systematic uncertainty affecting the muon elliptic flow measurement are considered. These take into account the changes due to the variations of the reference particle selection criteria as in [33,34,50], to allow us to check the robustness of the v_2^{μ} measurement. Since the collision impact parameter distribution could slightly depend on the observable used for the centrality determination, a systematic uncertainty is estimated by repeating the analysis using the number of clusters in the outermost layer of the SPD and the number of tracks in the TPC as centrality estimators, instead of the V0 signal amplitude. The systematic uncertainty due to the effect of TPC tracks from different Pb–Pb collisions piled-up in the same recorded event is estimated by applying a tighter cut to remove outliers in the multiplicity distribution of reference particles. This is done by requiring that the centrality values determined using the V0 signal amplitude and the number of TPC tracks do not differ by more than 5%. An additional systematic uncertainty specific to the scalar product is evaluated by varying the η gap between the two sub-events from 1 to 0.8 η-units (see Eq. (4) and [36]). The various systematic uncertainties are added in quadrature. They tend to increase with increasing p_T (see Fig. 1). A summary of the systematic uncertainties, in the interval $3 < p_T < 4.5$ GeV/c, is presented in Table 1.

Fig. 1 shows the p_T-differential muon elliptic flow (v_2^{μ}) in the 0–10%, 10–20% and 20–40% centrality classes as obtained using the various methods. The values of v_2^{μ} slightly increase from central to semi-central collisions and this effect is more pronounced in the p_T interval $3 < p_T < 4.5$ GeV/c. The two-particle correlation methods (scalar product and two-particle Q cumulants) give consistent results over the whole p_T range, indicating that these methods have a similar sensitivity to non-flow effects[3] and in particular to flow fluctuations. A similar agreement is found when comparing the multi-particle correlation methods (four-particle Q cumulants and Lee–Yang zeros) to each other. No significant difference between the v_2^{μ} results extracted with Lee–Yang zeros using either the sum or product generating function is seen, hence indicating that interferences between harmonics are negligible [51]. Moreover, four-particle Q cumulants give comparable results as Lee–Yang zeros. The four-particle Q cumulants and Lee–Yang zeros are expected to be less affected by non-flow effects than scalar product or two-particle Q cumulants [52]. However, as mentioned non-flow effects are expected to be negligible, even with two-particle correlation techniques, due to the large η between reference particles and inclusive muons. Finally, the central values of v_2^{μ} obtained with four-particle Q cumulants or Lee–Yang zeros are systematically smaller than with two-particle correlation methods, although compatible within uncertainties. Such differences may indicate that initial fluctuations play a role in the development of the final momentum-space anisotropy.

3.4. Muon background subtraction

The subtraction of the muon background contribution to the measured v_2^{μ} requires an estimate of the elliptic flow of muons from charged pion and kaon decays, $v_2^{\mu\leftarrow\pi,\mathrm{K}}$, and of the background fraction, $f^{\mu\leftarrow\pi,\mathrm{K}}$ (see Eq. (2)). The determination of the $v_2^{\mu\leftarrow\pi,\mathrm{K}}$ coefficient requires two steps. First, the p_T- and η-differential v_2 of charged particles measured in $|\eta| < 2.5$ by the ATLAS Collaboration in Pb–Pb collisions [53] and the p_T distributions of charged pions and kaons measured in $|y| < 0.8$ by

[3] Note that, in this analysis, most non-flow correlations are suppressed, even with two-particle correlation methods since reference particles and inclusive muons are separated by at least 1.7 η-units. However, it is worth mentioning that the main difference between the two methods is the η gap between the two sub-samples used to compute $\vec{Q}_2$ (Eq. (4)) which also allows to partly remove non-flow effects.

Table 1
Systematic uncertainty sources affecting the inclusive muon elliptic flow measurement in the 0–10%, 10–20% and 20–40% centrality classes for the interval $3 < p_{\mathrm{T}} < 4.5$ GeV/c. They are given as a percentage of the v_2 value.

v_2^{μ} analysis	Source	Systematic uncertainty (%) 0–10%	10–20%	20–40%
$v_2^{\mu}\{\mathrm{SP}\}$	Reference particles	3	1	3
	Centrality selection	6	1	4
	TPC pile-up	2	4	2
	η gap	13	1	1
$v_2^{\mu}\{2\}$	Reference particles	13	3	2
	Centrality selection	14	3	6
	TPC pile-up	8	1	4
$v_2^{\mu}\{4\}$	Reference particles			10
	Centrality selection			1
	TPC pile-up			1
$v_2^{\mu}\{\mathrm{LYZ\text{-}Sum}\}$	Reference particles			4
	Centrality selection			7
	TPC pile-up			2
$v_2^{\mu}\{\mathrm{LYZ\text{-}Prod}\}$	Reference particles			2
	Centrality selection			8
	TPC pile-up			2

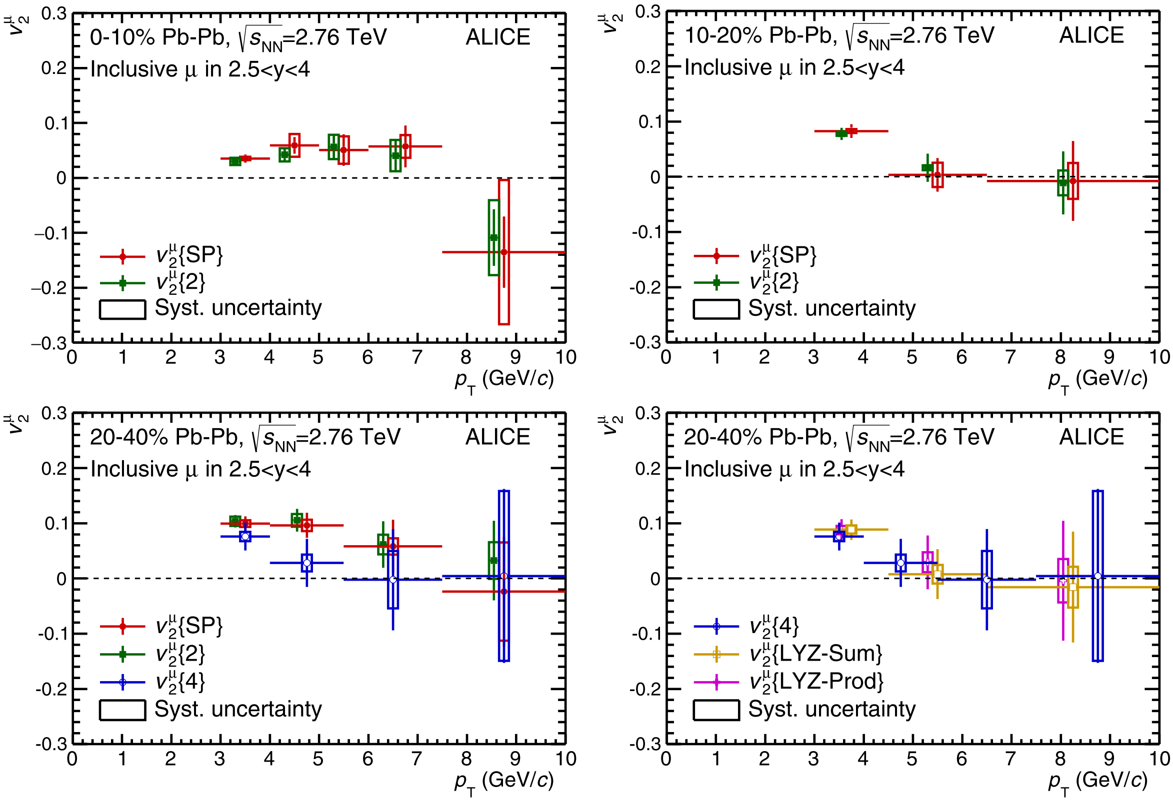

Fig. 1. p_{T}-differential inclusive muon v_2 in $2.5 < y < 4$ and various centrality intervals, in Pb–Pb collisions at $\sqrt{s_{\mathrm{NN}}} = 2.76$ TeV. The symbols are placed at the centre of the p_{T} interval and, for visibility, the points from two-particle Q cumulants and Lee–Yang zeros with product generating function are shifted horizontally. The vertical error bars represent the statistical uncertainty, the horizontal error bars correspond to the width of the bin (not shown for the shifted data points) and the open boxes are the systematic uncertainties. The p_{T} intervals used with the Lee–Yang zeros method are different with respect to the other methods. Upper panels: results from two-particle correlation flow methods (scalar product and two-particle Q cumulants) in the 0–10% (left) and 10–20% (right) centrality intervals. Lower panels: results in the 20–40% centrality interval from two-particle correlation flow methods (scalar product and two-particle Q cumulants) and from four-particle Q cumulants (left), and from four-particle Q cumulants and Lee–Yang zeros (right).

the ALICE Collaboration in pp and Pb–Pb collisions [54,55] are extrapolated to forward rapidity. Then, the p_{T} distributions of muons from charged pion and kaon decays, needed to estimate $f^{\mu\leftarrow\pi,\mathrm{K}}$ and $v_2^{\mu\leftarrow\pi,\mathrm{K}}$, are generated according to a simulation taking into account the decay kinematics and the effect of the front absorber.

The p_{T}- and η-differential elliptic flow of charged particles in $|\eta| < 2.5$, v_2^{ch}, is extrapolated to forward rapidity using:

$$v_2^{\mathrm{ch}}(p_{\mathrm{T}}, \eta) = F(\eta) \cdot v_2^{\mathrm{ch}}(p_{\mathrm{T}}, 2 < |\eta| < 2.5), \tag{9}$$

where $v_2^{\mathrm{ch}}(p_{\mathrm{T}}, 2 < |\eta| < 2.5)$ is the measured charged-particle elliptic flow in $2 < |\eta| < 2.5$ with the event plane method. Since the $v_2^{ch}(p_T)$ measured by the ATLAS Collaboration is affected by statistical fluctuations, it is assumed that in the interval $10 < p_T < 20$ GeV/c, needed to simulate the decay muons up to $p_T = 10$ GeV/c, v_2^{ch} remains constant with a value given by the one measured in the interval $10 < p_T < 12$ GeV/c. The extrapolation factor $F(\eta)$ is calculated by parameterizing the η-differential v_2^{ch} measured by the ATLAS Collaboration in various p_T intervals with a second order polynomial. In the interval $7 < p_T < 20$ GeV/c, the ATLAS v_2^{ch} does not show a dependence on η in $|\eta| < 2.5$. Therefore, for $p_T > 7$ GeV/c, $F(\eta)$ is computed as the average between a flat extrapolation function and the extrapolation factor obtained with the parabolic parameterization in $4 < p_T < 7$ GeV/c.

The mid-rapidity charged pion and kaon p_T distributions measured in Pb–Pb collisions are extrapolated to forward rapidity using the same strategy as in [21] and summarized in the following. Assuming that the nuclear modification factor $R_{AA}^{\pi,K}$ of charged pions and kaons in Pb–Pb collisions does not depend on rapidity up to $y = 4$ [21,56], the p_T distributions of charged pions and kaons at forward rapidity can be expressed as:

$$\frac{dN_{PbPb}^{\pi,K}}{dp_T dy} = \langle T_{AA}\rangle \cdot \frac{d\sigma_{pp}^{\pi,K}}{dp_T dy} \cdot [R_{AA}^{\pi,K}(p_T)]_{y=0}, \tag{10}$$

where $\langle T_{AA}\rangle$ is the average nuclear overlap function in centrality classes under study, estimated as described in [57]. The systematic uncertainty introduced by the assumption on $R_{AA}^{\pi,K}$ will be discussed later. The rapidity extrapolation of the mid-rapidity pion and kaon p_T-differential cross sections measured in pp collisions [21,58] is done according to:

$$\frac{d^2\sigma_{pp}^{\pi,K}}{dp_T dy} = \left[\frac{d^2\sigma_{pp}^{\pi,K}}{dp_T dy}\right]_{y=0} \cdot \exp\left(\frac{-y^2}{2\sigma_y^2}\right), \tag{11}$$

σ_y being estimated from Monte-Carlo event generators (see [21] for details).

The elliptic flow of muons from charged pion and kaon decays, $v_2^{\mu\leftarrow\pi,K}$, in $2.5 < y < 4$ and in various centrality classes,[4] is obtained by means of fast simulations using $v_2^{ch}(\eta, p_T)$ given by Eq. (9) and charged pion and kaon p_T distributions as obtained from Eqs. (10)–(11). The absorber effect is accounted for by rejecting the pions and kaons that do not decay within a distance corresponding to one interaction length from the beginning of the absorber. The simulation was repeated twice, considering that charged particles are either all pions or all kaons.

The background fraction, $f^{\mu\leftarrow\pi,K}$, is calculated as the ratio of the p_T-differential yield of muons from charged pion and kaon decays in $2.5 < y < 4$ obtained in the simulation to the measured p_T-differential yield of inclusive muons.

The systematic uncertainties affecting the estimated $v_2^{\mu\leftarrow\pi,K}$ are summarized in Table 2. They originate from i) the method used to measure the charged-particle v_2^{ch} in ATLAS, ii) the η and p_T extrapolation of v_2^{ch} and iii) the treatment of the charged-particle v_2^{ch} in the fast simulation procedure. As the event plane method was used for the v_2^{ch} measurement in ATLAS, the results range between the mean ($\langle v_2^{ch}\rangle$) and R.M.S. ($\sqrt{\langle (v_2^{ch})^2\rangle}$) of the true v_2^{ch} values due to fluctuations, depending on the event plane resolution which varies with the collision centrality [49]. According to a Monte-Carlo Glauber model [49], the ratio $\sqrt{\langle v_2^2\rangle}/\langle v_2\rangle$ is expected

[4] The $v_2^{\mu\leftarrow\pi,K}$ of muons from charged pion and kaon decays in the 20–40% centrality class is then obtained from the mean of the charged-particle v_2 in 20–30% and 30–40% centrality classes, with an additional systematic uncertainty provided by the difference with respect to the results in these two centrality classes.

Table 2
Systematic uncertainty sources affecting the estimated $v_2^{\mu\leftarrow\pi,K}$ for the interval $3 < p_T < 10$ GeV/c. They are stated as a percentage of the v_2 value. The given range reflects the dependence on the collision centrality.

Source	Systematic uncertainty (%)
Input v_2^{ch} bias	9
v_2^{ch} η extrapolation	9–12
v_2^{ch} high p_T extrapolation	13–15
π and K in fast simulations	< 1

to vary from about 1.06 to 1.15. Consequently, a conservative systematic uncertainty of 15% is applied to account for this bias and is propagated to $v_2^{\mu\leftarrow\pi,K}$. The systematic uncertainty due to the η extrapolation of v_2^{ch} is evaluated using several fit functions (first and third order polynomials, and Gaussian function) in the region $p_T < 7$ GeV/c, and for larger p_T values an additional systematic uncertainty due to the extrapolation procedure is considered. The latter is determined by comparing the results obtained with the two extrapolation functions used in the interval $p_T > 7$ GeV/c. The systematic uncertainty due to the assumption on v_2^{ch} in the region $p_T > 10$ GeV/c is estimated by varying v_2^{ch} between 0 and the value in $10 < p_T < 12$ GeV/c in the fast simulations. Such uncertainty affects mainly the high p_T region ($p_T > 7$ GeV/c). Finally, the systematic uncertainty obtained by treating charged particles separately as pions and kaons is found to be negligible. The various systematic uncertainty sources are propagated to the estimated $v_2^{\mu\leftarrow\pi,K}$ and added in quadrature.

The systematic uncertainty on $f^{\mu\leftarrow\pi,K}$, detailed in [21], includes the uncertainty on the generated p_T distributions of muons from charged pion and kaon decays, and the uncertainty on the measured inclusive muon p_T distributions. The former originates from the input charged pion and kaon distributions, the rapidity extrapolation and the absorber effect. The systematic uncertainty on the measured inclusive muon yields contains the systematic uncertainty on detector response, residual mis-alignment and centrality dependence of the efficiency. This gives a total systematic uncertainty on $f^{\mu\leftarrow\pi,K}$ of about 21% in the interval $3 < p_T < 4.5$ GeV/c with almost no dependence on the collision centrality. Finally, as done for the measurement of the heavy-flavour decay muon R_{AA} [21], the systematic uncertainty due to the unknown suppression of charged particles at forward rapidity is calculated by varying $f^{\mu\leftarrow\pi,K}$ from 0 to two times the estimated value. This corresponds to a variation of $R_{AA}^{\pi,K}(p_T)$ at forward rapidity from 0 up to two times $[R_{AA}^{\pi,K}(p_T)]_{y=0}$. This systematic uncertainty amounts to 10–30% in the interval $3 < p_T < 4.5$ GeV/c, depending on the collision centrality and the flow analysis method.

Fig. 2 presents the estimated background elliptic flow ($v_2^{\mu\leftarrow\pi,K}$, left) and background fraction ($f^{\mu\leftarrow\pi,K}$, right) as a function of p_T in the 0–10%, 10–20% and 20–40% centrality classes. The open boxes represent the systematic uncertainties previously discussed, except for the systematic uncertainty due to the unknown suppression of charged particles at forward rapidity which is treated separately. The estimated $v_2^{\mu\leftarrow\pi,K}$ and $f^{\mu\leftarrow\pi,K}$ decrease with increasing p_T. A decreasing trend of the magnitude of $v_2^{\mu\leftarrow\pi,K}$ from semi-central collisions towards central collisions is also observed.

Finally, the systematic uncertainty on the elliptic flow of muons from heavy-flavour decays, $v_2^{\mu\leftarrow HF}$, contains two contributions: the systematic uncertainties on v_2^{μ}, $v_2^{\mu\leftarrow\pi,K}$ and $f^{\mu\leftarrow\pi,K}$ propagated according to the definition of $v_2^{\mu\leftarrow HF}$ given in Eq. (2), and the systematic uncertainty due to the unknown suppression of charged particles at forward rapidity. The final systematic uncertainty on $v_2^{\mu\leftarrow HF}$ is obtained by adding in quadrature the two contributions.

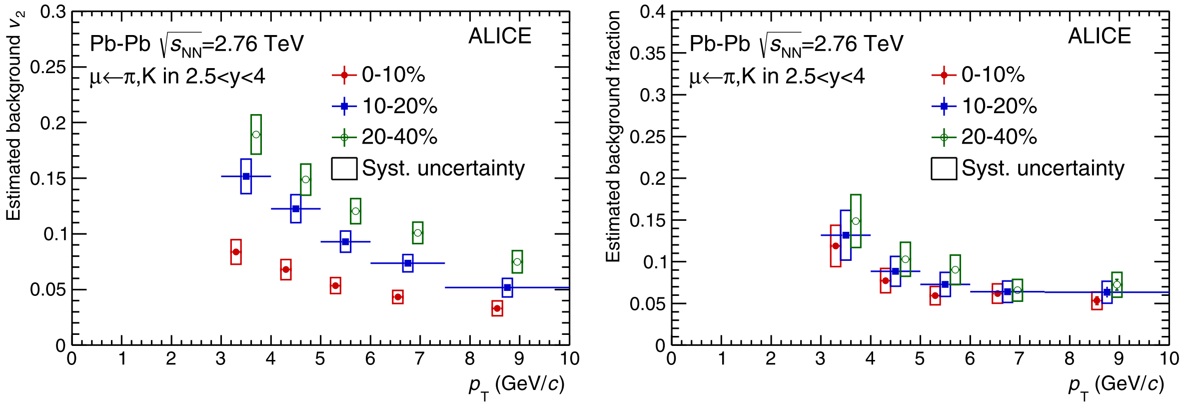

Fig. 2. Estimated background v_2 ($v_2^{\mu\leftarrow\pi,K}$, left) and background fraction ($f^{\mu\leftarrow\pi,K}$, right) as a function of p_T in $2.5 < y < 4$ and various centrality intervals, in Pb–Pb collisions at $\sqrt{s_{NN}} = 2.76$ TeV. The symbols are placed at the centre of the p_T interval and, for visibility, the points for the centrality classes 10–20% and 20–40% are shifted horizontally. The horizontal error bars correspond to the width of the bin (not shown for the shifted values) and the open boxes are the systematic uncertainties. See the text for details.

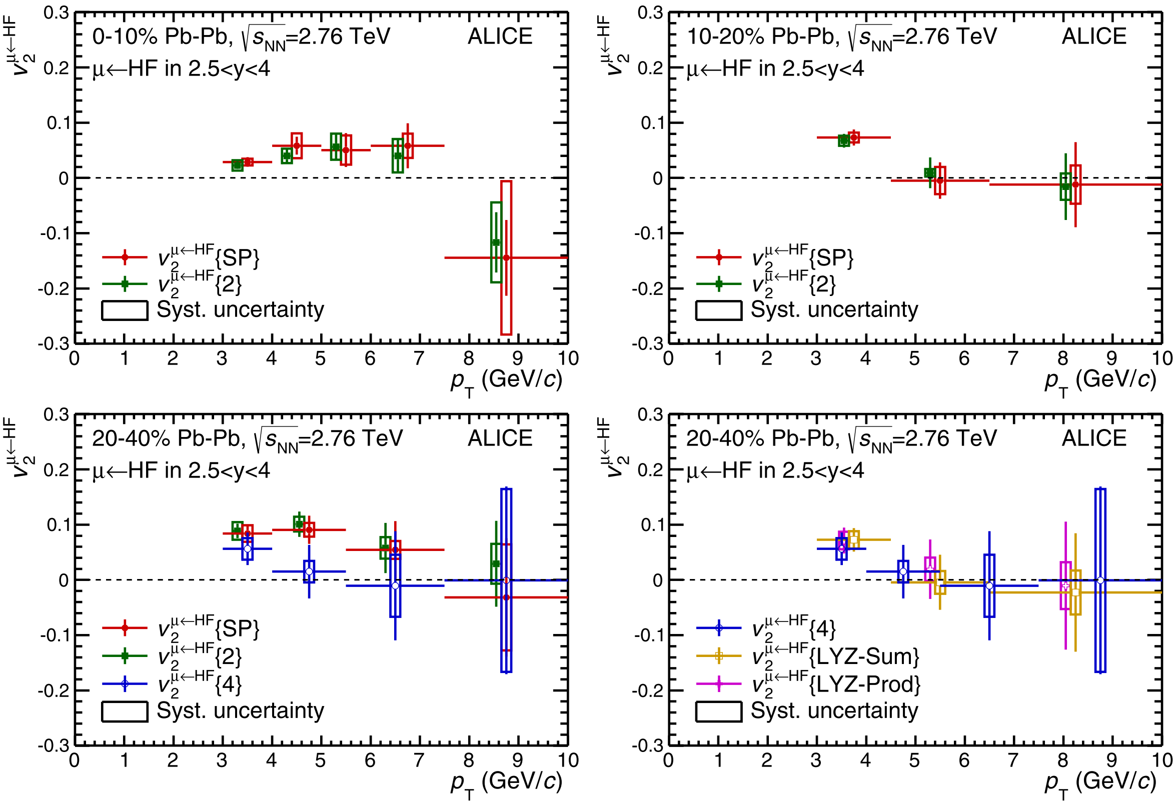

Fig. 3. p_T-differential elliptic flow of muons from heavy-flavour decays, $v_2^{\mu\leftarrow HF}$, in $2.5 < y < 4$ and various centrality intervals, in Pb–Pb collisions at $\sqrt{s_{NN}} = 2.76$ TeV. The symbols are placed at the centre of the p_T interval and, for visibility, the points from two-particle Q cumulants and Lee–Yang zeros with product generating function are shifted horizontally. The meaning of the symbols is the same as in Fig. 1. The horizontal error bars are not plotted for shifted data points. The p_T intervals used with the Lee–Yang zeros method are different with respect to the other methods. Upper panels: results from two-particle correlation flow methods (scalar product and two-particle Q cumulants) in the 0–10% (left) and 10–20% (right) centrality intervals. Lower panels: results in the 20–40% centrality interval from two-particle correlation flow methods (scalar product and two-particle Q cumulants) and from four-particle Q cumulants (left), and from four-particle Q cumulants and Lee–Yang zeros (right). See the text for details.

It amounts to about 12%–36% in the interval $3 < p_T < 4.5$ GeV/c, depending on the collision centrality and the flow analysis method.

4. Results

Fig. 3 presents the p_T-differential elliptic flow of muons from heavy-flavour hadron decays, $v_2^{\mu\leftarrow HF}$, calculated with Eq. (2). The results are shown for the 0–10% (upper, left), 10–20% (upper, right) and 20–40% (bottom) centrality classes using the same flow methods as for the measurement of the inclusive muon elliptic flow (Fig. 1). When comparing the results to those obtained for inclusive muons (Fig. 1), one can notice that $v_2^{\mu\leftarrow HF}$ and v_2^{μ} are similar due to the small background fraction (5% to 15%) in the p_T interval 3–10 GeV/c. The differences between the various methods are similar to those discussed for the measurement of the inclusive muon v_2^{μ} i.e. i) scalar product and two-particle Q cumulants give compatible results, ii) consistent results are also found with four-particle Q cumulants and Lee–Yang zeros, and iii) the $v_2^{\mu\leftarrow HF}$ values extracted from these multi-particle correlation methods are smaller, although still compatible within un-

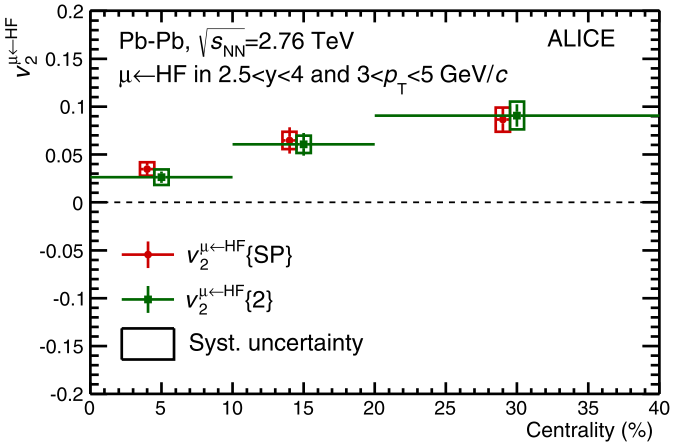

Fig. 4. Elliptic flow of muons from heavy-flavour hadron decays as a function of the collision centrality in $2.5 < y < 4$ and $3 < p_T < 5$ GeV/c, in Pb–Pb collisions at $\sqrt{s_{NN}} = 2.76$ TeV. The results are obtained with scalar product and two-particle Q cumulants. Vertical bars (open boxes) represent the statistical (systematic) uncertainty, the horizontal error bars correspond to the width of the centrality bin. For visibility, the points from scalar product are shifted horizontally and the horizontal error bars are not plotted.

certainties, than the ones obtained with two-particle correlation methods. As mentioned in Section 3.3, such differences are expected if initial-state fluctuations play a role in the development of the final momentum-space anisotropy.

A positive $v_2^{\mu\leftarrow HF}$ is observed at intermediate p_T for the 20–40% and 10–20% centrality classes with a significance larger than 3σ when combining statistical and systematic uncertainties. In the 20–40% centrality class, the values of the significance in the interval $3 < p_T < 4$ GeV/c ($4 < p_T < 5.5$ GeV/c) are 4σ (3.2σ) and 4.3σ (3.8σ) with scalar product and two-particle Q cumulants, respectively. In the 10–20% centrality class and in the interval $3 < p_T < 4.5$ GeV/c, the values of the significance correspond to 4.4σ both with scalar product and two-particle Q cumulants. This behavior results from the interplay between the significant interaction of heavy quarks with the expanding medium and the path-length dependence of in-medium parton energy loss [29,30]. The $v_2^{\mu\leftarrow HF}$ of muons from heavy-flavour hadron decays decreases with increasing p_T and becomes compatible with zero in the high p_T region.

Fig. 4 shows the centrality dependence of the elliptic flow of muons from heavy-flavour hadron decays in the interval $3 < p_T < 5$ GeV/c. It is investigated with scalar product and two-particle Q cumulants, which can be applied in a wider event-multiplicity (i.e. centrality) interval compared to multi-particle correlation methods. A significant decrease of the v_2 magnitude towards central collisions is observed. This is expected from the decrease of the initial spatial anisotropy from semi-central to central collisions.

ALICE has measured the elliptic flow of prompt D mesons in $|y| < 0.8$ in three centrality classes in the interval 0–50% with various two-particle correlation methods [33,34]. Similar trends as those reported here for muons from heavy-flavour decays are observed, although in different p_T and rapidity intervals. In particular, a positive v_2 was observed for D mesons in semi-central collisions in $2 < p_T < 6$ GeV/c with a significance of 5.7σ.

The positive elliptic flow of muons from heavy-flavour hadron decays has been observed in a p_T interval from 3 to about 5 GeV/c where the charm contribution is expected to be dominant with respect to the beauty component according to perturbative QCD calculations [21]. This measurement supports the interpretation of the J/ψ positive v_2 at forward rapidity [35] in terms of a significant contribution to J/ψ production from recombination of flowing charm quarks in the deconfined medium.

5. Comparison with models

The results presented in this publication may constrain models describing the interactions of heavy quarks with the medium via elastic (collisional) and inelastic (radiative) processes, and in particular the parton energy loss dependence on the path-length within the medium.

The elliptic flow coefficient and the nuclear modification factor of muons from heavy-flavour hadron decays [21] are compared to the following three models. The MC@sHQ + EPOS transport model [59] treats the propagation of heavy quarks in the medium including collisional and radiative energy loss, within a 3 + 1 dimensional fluid dynamical expansion based on the EPOS model [60,61]. The hadronization of heavy quarks takes place at the transition temperature via recombination at low p_T and fragmentation at intermediate and high p_T. The final-state hadronic interactions are not included in the model. TAMU [62] is a transport model including only collisional processes via the Langevin equation. The hydrodynamical expansion is constrained by p_T spectra and elliptic flow data of light-flavour hadrons. The hadronization is modeled including a component of recombination of heavy quarks with light-flavour hadrons in the QGP. The diffusion of heavy-flavour mesons in the hadronic phase is also included. BAMPS [63–65] is a partonic transport model based on the Boltzmann approach to multi-parton scatterings. It includes collisional processes with a running strong coupling constant. The lack of radiative contributions is accounted for by scaling the binary cross section with a correction factor, tuned to describe the nuclear modification factor and elliptic flow results at RHIC energies. Vacuum fragmentation functions are used for the hadronization.

Fig. 5 shows a comparison of the three models with the measurement of the p_T-differential elliptic flow of muons from heavy-flavour hadron decays in the 20–40% centrality class (upper panel) and of the p_T-differential nuclear modification factor of muons from heavy-flavour hadron decays in the 0–10% centrality class [21] (lower panel). In the interval $3 < p_T < 5$ GeV/c, the BAMPS model describes the $v_2^{\mu\leftarrow HF}$ data within uncertainties, while the TAMU and MC@sHQ+EPOS models give $v_2^{\mu\leftarrow HF}$ values lower than the data. The three models describe the $v_2^{\mu\leftarrow HF}$ data at higher p_T, although the sizeable experimental uncertainties affect the significance of the comparison. The BAMPS model tends to slightly underestimate the R_{AA} of muons from heavy-flavour decays in the 10% most central collisions, while the MC@sHQ+EPOS

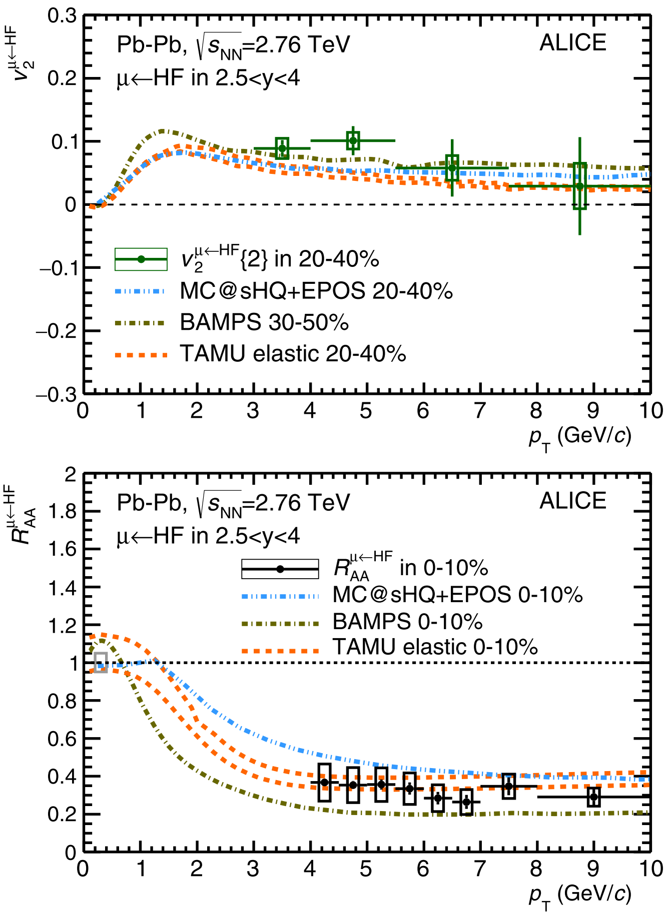

Fig. 5. Upper panel: p_T-differential elliptic flow of muons from heavy-flavour hadron decays in $2.5 < y < 4$, in Pb–Pb collisions at $\sqrt{s_{NN}} = 2.76$ TeV for the centrality class 20–40% compared to various transport model predictions: MC@sHQ + EPOS [59–61], TAMU [62] and BAMPS [63–65]. The TAMU model is shown with a theoretical uncertainty band. Lower panel: p_T-differential R_{AA} of muons from heavy-flavour hadron decays for the centrality class 0–10% from [21] compared to the same models as for $v_2^{\mu\leftarrow HF}$.

model tends to overestimate it. The TAMU model describes the R_{AA} measurement over the entire p_T interval within uncertainties. These comparisons indicate that it is challenging to simultaneously describe the strong suppression of high-p_T muons from heavy-flavour hadron decays in central collisions and the azimuthal anisotropy in semi-central collisions. Similar trends are also observed in the mid-rapidity region from the comparison of the R_{AA} and v_2 of D mesons with model calculations [34].

6. Conclusions

In summary, we have reported on a measurement of the elliptic flow of muons from heavy-flavour hadron decays at forward rapidity in central and semi-central Pb–Pb collisions at $\sqrt{s_{NN}} = 2.76$ TeV with the ALICE detector at the LHC.

Measurements have been carried out using several methods which exhibit different sensitivity to initial-state fluctuations and non-flow correlations. The systematic comparison of scalar product, two- and four-particle Q cumulants and Lee–Yang zeros helps in understanding the processes that build up the observed differences between two-particle correlation methods and multi-particle correlation methods and suggests that flow fluctuations are significant.

The magnitude of the elliptic flow of muons from heavy-flavour hadron decays increases from central to semi-central collisions and decreases with increasing p_T, becoming compatible with zero at high p_T. The results indicate a positive elliptic flow with the scalar product and two-particle Q cumulants in semi-central collisions (10–20% and 20–40% centrality classes) for the p_T interval from 3 to about 5 GeV/c with a significance larger than 3σ. The elliptic flow in semi-central collisions and the previously published nuclear modification factor in the 10% most central collisions were compared with transport model calculations. These comparisons show that a simultaneous description of R_{AA} and v_2 over the whole p_T interval remains a challenge. The results reported in this Letter in various centrality classes may provide further important constraints to the models.

Acknowledgements

The ALICE Collaboration would like to thank all its engineers and technicians for their invaluable contributions to the construction of the experiment and the CERN accelerator teams for the outstanding performance of the LHC complex. The ALICE Collaboration gratefully acknowledges the resources and support provided by all Grid centres and the Worldwide LHC Computing Grid (WLCG) collaboration. The ALICE Collaboration acknowledges the following funding agencies for their support in building and running the ALICE detector: State Committee of Science, World Federation of Scientists (WFS) and Swiss Fonds Kidagan, Armenia; Conselho Nacional de Desenvolvimento Científico e Tecnológico (CNPq), Financiadora de Estudos e Projetos (FINEP), Fundação de Amparo à Pesquisa do Estado de São Paulo (FAPESP); National Natural Science Foundation of China (NSFC), the Chinese Ministry of Education (CMOE) and the Ministry of Science and Technology of China (MSTC); Ministry of Education and Youth of the Czech Republic; Danish Natural Science Research Council, the Carlsberg Foundation and the Danish National Research Foundation; The European Research Council under the European Community's Seventh Framework Programme; Helsinki Institute of Physics and the Academy of Finland; French CNRS-IN2P3, the 'Region Pays de Loire', 'Region Alsace', 'Region Auvergne' and CEA, France; German Bundesministerium für Bildung, Wissenschaft, Forschung und Technologie (BMBF) and the Helmholtz Association; General Secretariat for Research and Technology, Ministry of Development, Greece; National Research, Development and Innovation Office (NKFIH), Hungary; Department of Atomic Energy and Department of Science and Technology of the Government of India; Istituto Nazionale di Fisica Nucleare (INFN) and Centro Fermi – Museo Storico della Fisica e Centro Studi e Ricerche "Enrico Fermi", Italy; Japan Society for the Promotion of Science (JSPS) KAKENHI and MEXT, Japan; Joint Institute for Nuclear Research, Dubna; National Research Foundation of Korea (NRF); Consejo Nacional de Cienca y Tecnologia (CONACYT), Direccion General de Asuntos del Personal Academico (DGAPA), México, Amerique Latine Formation academique – European Commission (ALFA-EC) and the EPLANET Program (European Particle Physics Latin American Network); Stichting voor Fundamenteel Onderzoek der Materie (FOM) and the Nederlandse Organisatie voor Wetenschappelijk Onderzoek (NWO), Netherlands; Research Council of Norway (NFR); National Science Centre, Poland; Ministry of National Education/Institute for Atomic Physics and National Council of Scientific Research in Higher Education (CNCSI-UEFISCDI), Romania; Ministry of Education and Science of Russian Federation, Russian Academy of Sciences, Russian Federal Agency of Atomic Energy, Russian Federal Agency for Science and Innovations and The Russian Foundation for Basic Research; Ministry of Education of Slovakia; Department of Science and Technology, South Africa; Centro de Investigaciones Energeticas, Medioambientales y Tecnologicas (CIEMAT), E-Infrastructure shared between Europe and Latin America (EELA), Ministerio de Economía y Competitividad

(MINECO) of Spain, Xunta de Galicia (Consellería de Educación), Centro de Aplicaciones Tecnológicas y Desarrollo Nuclear (CEADEN), Cubaenergía, Cuba, and IAEA (International Atomic Energy Agency); Swedish Research Council (VR) and Knut & Alice Wallenberg Foundation (KAW); Ukraine Ministry of Education and Science; United Kingdom Science and Technology Facilities Council (STFC); The United States Department of Energy, the United States National Science Foundation, the State of Texas, and the State of Ohio; Ministry of Science, Education and Sports of Croatia and Unity through Knowledge Fund, Croatia; Council of Scientific and Industrial Research (CSIR), New Delhi, India; Pontificia Universidad Católica del Perú.

References

[1] F. Karsch, Lattice simulations of the thermodynamics of strongly interacting elementary particles and the exploration of new phases of matter in relativistic heavy ion collisions, J. Phys. Conf. Ser. 46 (2006) 122–131, arXiv:hep-lat/0608003.
[2] Wuppertal-Budapest Collaboration, S. Borsanyi, et al., Is there still any T_c mystery in lattice QCD? Results with physical masses in the continuum limit III, J. High Energy Phys. 1009 (2010) 073, arXiv:1005.3508 [hep-lat].
[3] S. Borsanyi, G. Endrodi, Z. Fodor, A. Jakovac, S.D. Katz, et al., The QCD equation of state with dynamical quarks, J. High Energy Phys. 1011 (2010) 077, arXiv:1007.2580 [hep-lat].
[4] A. Bazavov, T. Bhattacharya, M. Cheng, C. DeTar, H. Ding, et al., The chiral and deconfinement aspects of the QCD transition, Phys. Rev. D 85 (2012) 054503, arXiv:1111.1710 [hep-lat].
[5] P. Petreczky, Review of recent highlights in lattice calculations at finite temperature and finite density, PoS ConfinementX (2012) 028, arXiv:1301.6188 [hep-lat].
[6] M. Gyulassy, M. Plumer, Jet quenching in dense matter, Phys. Lett. B 243 (1990) 432–438.
[7] R. Baier, Y.L. Dokshitzer, A.H. Mueller, S. Peigne, D. Schiff, Radiative energy loss and p_T broadening of high-energy partons in nuclei, Nucl. Phys. B 484 (1997) 265–282, arXiv:hep-ph/9608322.
[8] M.H. Thoma, M. Gyulassy, Quark damping and energy loss in the high temperature QCD, Nucl. Phys. B 351 (1991) 491–506.
[9] E. Braaten, M.H. Thoma, Energy loss of a heavy fermion in a hot plasma, Phys. Rev. D 44 (1991) 1298–1310.
[10] E. Braaten, M.H. Thoma, Energy loss of a heavy quark in the quark–gluon plasma, Phys. Rev. D 44 (1991) 2625–2630.
[11] PHENIX Collaboration, K. Adcox, et al., Measurement of single electrons and implications for charm production in Au + Au collisions at $\sqrt{s_{NN}} = 130$ GeV, Phys. Rev. Lett. 88 (2002) 192303, arXiv:nucl-ex/0202002.
[12] PHENIX Collaboration, S. Adler, et al., Centrality dependence of charm production from single electrons measurement in Au + Au collisions at $\sqrt{s_{NN}} = 200$ GeV, Phys. Rev. Lett. 94 (2005) 082301, arXiv:nucl-ex/0409028.
[13] PHENIX Collaboration, S. Adler, et al., Nuclear modification of electron spectra and implications for heavy quark energy loss in Au + Au collisions at $\sqrt{s_{NN}} = 200$ GeV, Phys. Rev. Lett. 96 (2006) 032301, arXiv:nucl-ex/0510047.
[14] PHENIX Collaboration, A. Adare, et al., Energy loss and flow of heavy quarks in Au + Au collisions at $\sqrt{s_{NN}} = 200$ GeV, Phys. Rev. Lett. 98 (2007) 172301, arXiv:nucl-ex/0611018.
[15] PHENIX Collaboration, A. Adare, et al., Heavy quark production in p + p and energy loss and flow of heavy quarks in Au + Au collisions at $\sqrt{s_{NN}} = 200$ GeV, Phys. Rev. C 84 (2011) 044905, arXiv:1005.1627 [nucl-ex].
[16] PHENIX Collaboration, A. Adare, et al., System-size dependence of open-heavy-flavor production in nucleus–nucleus collisions at $\sqrt{s_{NN}} = 200$ GeV, Phys. Rev. C 90 (3) (2014) 034903, arXiv:1310.8286 [nucl-ex].
[17] STAR Collaboration, B. Abelev, et al., Transverse momentum and centrality dependence of high-p_T non-photonic electron suppression in Au + Au collisions at $\sqrt{s_{NN}} = 200$ GeV, Phys. Rev. Lett. 98 (2007) 192301, arXiv:nucl-ex/0607012; STAR Collaboration, B. Abelev, et al., Phys. Rev. Lett. 106 (2011) 159902 (Erratum).
[18] STAR Collaboration, L. Adamczyk, et al., Observation of D^0 meson nuclear modifications in Au + Au collisions at $\sqrt{s_{NN}} = 200$ GeV, Phys. Rev. Lett. 113 (14) (2014) 142301, arXiv:1404.6185 [nucl-ex].
[19] PHENIX Collaboration, A. Adare, et al., Nuclear-modification factor for open-heavy-flavor production at forward rapidity in Cu + Cu collisions at $\sqrt{s_{NN}} = 200$ GeV, Phys. Rev. C 86 (2012) 024909, arXiv:1204.0754 [nucl-ex].
[20] ALICE Collaboration, B. Abelev, et al., Suppression of high transverse momentum D mesons in central Pb–Pb collisions at $\sqrt{s_{NN}} = 2.76$ TeV, J. High Energy Phys. 1209 (2012) 112, arXiv:1203.2160 [nucl-ex].
[21] ALICE Collaboration, B. Abelev, et al., Production of muons from heavy flavour decays at forward rapidity in pp and Pb–Pb collisions at $\sqrt{s_{NN}} = 2.76$ TeV, Phys. Rev. Lett. 109 (2012) 112301, arXiv:1205.6443 [hep-ex].
[22] CMS Collaboration, J/ψ results from CMS in Pb–Pb collisions, with 150 μb^{-1} data, Tech. Rep. CMS-PAS-HIN-12-014, CERN, Geneva, 2012, https://cds.cern.ch/record/1472735.
[23] CMS Collaboration, S. Chatrchyan, et al., Suppression of non-prompt J/ψ, prompt J/ψ, and Υ(1S) in Pb–Pb collisions at $\sqrt{s_{NN}} = 2.76$ TeV, J. High Energy Phys. 1205 (2012) 063, arXiv:1201.5069 [nucl-ex].
[24] ALICE Collaboration, J. Adam, et al., Inclusive, prompt and non-prompt J/ψ production at mid-rapidity in Pb–Pb collisions at $\sqrt{s_{NN}} = 2.76$ TeV, arXiv:1504.07151 [nucl-ex].
[25] S.A. Voloshin, A.M. Poskanzer, R. Snellings, in: Relativistic Heavy Ion Physics, in: Landolt–Boernstein New Series, vol. 1/23, Springer-Verlag, 2010, p. 5.
[26] J.-Y. Ollitrault, Anisotropy as a signature of transverse collective flow, Phys. Rev. D 46 (1992) 229–245.
[27] V. Greco, C. Ko, R. Rapp, Quark coalescence for charmed mesons in ultrarelativistic heavy ion collisions, Phys. Lett. B 595 (2004) 202–208, arXiv:nucl-th/0312100.
[28] A. Andronic, P. Braun-Munzinger, K. Redlich, J. Stachel, Statistical hadronization of charm in heavy ion collisions at SPS, RHIC and LHC, Phys. Lett. B 571 (2003) 36–44, arXiv:nucl-th/0303036.
[29] M. Gyulassy, I. Vitev, X. Wang, High p_T azimuthal asymmetry in noncentral A + A at RHIC, Phys. Rev. Lett. 86 (2001) 2537–2540, arXiv:nucl-th/0012092.
[30] E. Shuryak, The azimuthal asymmetry at large p_T seem to be too large for a 'jet quenching', Phys. Rev. C 66 (2002) 027902, arXiv:nucl-th/0112042.
[31] PHENIX Collaboration, S. Adler, et al., Measurement of single electron event anisotropy in Au + Au collisions at $\sqrt{s_{NN}} = 200$ GeV, Phys. Rev. C 72 (2005) 024901, arXiv:nucl-ex/0502009.
[32] STAR Collaboration, L. Adamczyk, et al., Elliptic flow of non-photonic electrons in Au + Au collisions at $\sqrt{s_{NN}} = 200$, 62.4 and 39 GeV, arXiv:1405.6348 [hep-ex].
[33] ALICE Collaboration, B. Abelev, et al., D meson elliptic flow in non-central Pb–Pb collisions at $\sqrt{s_{NN}} = 2.76$ TeV, Phys. Rev. Lett. 111 (2013) 102301, arXiv:1305.2707 [nucl-ex].
[34] ALICE Collaboration, B.B. Abelev, et al., Azimuthal anisotropy of D meson production in Pb–Pb collisions at $\sqrt{s_{NN}} = 2.76$ TeV, Phys. Rev. C 90 (3) (2014) 034904, arXiv:1405.2001 [nucl-ex].
[35] ALICE Collaboration, E. Abbas, et al., J/ψ elliptic flow in Pb–Pb collisions at $\sqrt{s_{NN}} = 2.76$ TeV, Phys. Rev. Lett. 111 (2013) 162301, arXiv:1303.5880 [nucl-ex].
[36] STAR Collaboration, C. Adler, et al., Elliptic flow from two and four particle correlations in Au + Au collisions at $\sqrt{s_{NN}} = 130$ GeV, Phys. Rev. C 66 (2002) 034904, arXiv:nucl-ex/0206001.
[37] N. Borghini, P.M. Dinh, J.-Y. Ollitrault, Flow analysis from multiparticle azimuthal correlations, Phys. Rev. C 64 (2001) 054901, arXiv:nucl-th/0105040.
[38] A. Bilandzic, R. Snellings, S. Voloshin, Flow analysis with cumulants: direct calculations, Phys. Rev. C 83 (2011) 044913, arXiv:1010.0233 [nucl-ex].
[39] R. Bhalerao, N. Borghini, J. Ollitrault, Analysis of anisotropic flow with Lee–Yang zeroes, Nucl. Phys. A 727 (2003) 373–426, arXiv:nucl-th/0310016.
[40] R. Bhalerao, N. Borghini, J. Ollitrault, Genuine collective flow from Lee–Yang zeroes, Phys. Lett. B 580 (2004) 157–162, arXiv:nucl-th/0307018.
[41] N. Borghini, R. Bhalerao, J. Ollitrault, Anisotropic flow from Lee–Yang zeroes: a practical guide, J. Phys. G 30 (2004) S1213–S1216, arXiv:nucl-th/0402053.
[42] ALICE Collaboration, K. Aamodt, et al., The ALICE experiment at the CERN LHC, J. Instrum. 3 (2008), S08002.
[43] ALICE Collaboration, B.B. Abelev, et al., Performance of the ALICE experiment at the CERN LHC, Int. J. Mod. Phys. A 29 (2014) 1430044, arXiv:1402.4476 [nucl-ex].
[44] ALICE Collaboration, B. Abelev, et al., Centrality dependence of π, K, p production in Pb–Pb collisions at $\sqrt{s_{NN}} = 2.76$ TeV, Phys. Rev. C 88 (2013) 044910, arXiv:1303.0737 [hep-ex].
[45] ALICE Collaboration, B. Abelev, et al., Heavy flavour decay muon production at forward rapidity in proton–proton collisions at $\sqrt{s} = 7$ TeV, Phys. Lett. B 708 (2012) 265–275, arXiv:1201.3791 [hep-ex].
[46] ALICE Collaboration, K. Aamodt, et al., Higher harmonic anisotropic flow measurements of charged particles in Pb–Pb collisions at $\sqrt{s_{NN}} = 2.76$ TeV, Phys. Rev. Lett. 107 (2011) 032301, arXiv:1105.3865 [nucl-ex].
[47] M. Luzum, Collective flow and long-range correlations in relativistic heavy ion collisions, Phys. Lett. B 696 (2011) 499–504, arXiv:1011.5773 [nucl-th].
[48] A.M. Poskanzer, S. Voloshin, Methods for analyzing anisotropic flow in relativistic nuclear collisions, Phys. Rev. C 58 (1998) 1671–1678, arXiv:nucl-ex/9805001.
[49] M. Luzum, J.-Y. Ollitrault, Eliminating experimental bias in anisotropic-flow measurements of high-energy nuclear collisions, Phys. Rev. C 87 (4) (2013) 044907, arXiv:1209.2323 [nucl-ex].
[50] ALICE Collaboration, B. Abelev, et al., Anisotropic flow of charged hadrons, pions and (anti-)protons measured at high transverse momentum in Pb–Pb collisions at $\sqrt{s_{NN}} = 2.76$ TeV, Phys. Lett. B 719 (2013) 18–28, arXiv:1205.5761 [nucl-ex].
[51] STAR Collaboration, B. Abelev, et al., Centrality dependence of charged hadron and strange hadron elliptic flow from $\sqrt{s_{NN}} = 200$ GeV Au + Au collisions, Phys. Rev. C 77 (2008) 054901, arXiv:0801.3466 [nucl-ex].

[52] CMS Collaboration, S. Chatrchyan, et al., Measurement of the elliptic anisotropy of charged particles produced in Pb–Pb collisions at $\sqrt{s_{NN}} = 2.76$ TeV, Phys. Rev. C 87 (1) (2013) 014902, arXiv:1204.1409 [nucl-ex].
[53] ATLAS Collaboration, G. Aad, et al., Measurement of the pseudorapidity and transverse momentum dependence of the elliptic flow of charged particles in lead–lead collisions at $\sqrt{s_{NN}} = 2.76$ TeV with the ATLAS detector, Phys. Lett. B 707 (2012) 330–348, arXiv:1108.6018 [hep-ex].
[54] ALICE Collaboration, P. Christiansen, Identified charged pion, kaon and proton-sin pp and Pb–Pb collisins at LHC energies measured with ALICE, PoS EPS-HEP 2013 (2013) 173.
[55] ALICE Collaboration, B.B. Abelev, et al., Production of charged pions, kaons and protons at large transverse momenta in pp and Pb–Pb collisions at $\sqrt{s_{NN}} = 2.76$ TeV, Phys. Lett. B 736 (2014) 196–207, arXiv:1401.1250 [nucl-ex].
[56] ATLAS Collaboration, A. Milov, Centrality dependence of charged particle spectra and R_{CP} in Pb + Pb collisions at $\sqrt{s_{NN}} = 2.76$ TeV with the ATLAS detector at the LHC, J. Phys. G 38 (2011) 124113, arXiv:1107.0460 [nucl-ex].
[57] ALICE Collaboration, B. Abelev, et al., Centrality determination of Pb–Pb collisions at $\sqrt{s_{NN}} = 2.76$ TeV with ALICE, Phys. Rev. C 88 (4) (2013) 044909, arXiv:1301.4361 [nucl-ex].
[58] PHENIX Collaboration, S. Adler, et al., Measurement of single muons at forward rapidity in p + p collisions at $\sqrt{s} = 200$ GeV and implications for charm production, Phys. Rev. D 76 (2007) 092002, arXiv:hep-ex/0609032.
[59] M. Nahrgang, J. Aichelin, P.B. Gossiaux, K. Werner, Influence of hadronic bound states above T_c on heavy-quark observables in Pb + Pb collisions at the CERN Large Hadron Collider, Phys. Rev. C 89 (1) (2014) 014905, arXiv:1305.6544 [hep-ph].
[60] K. Werner, I. Karpenko, T. Pierog, M. Bleicher, K. Mikhailov, Event-by-event simulation of the three-dimensional hydrodynamic evolution from flux tube initial conditions in ultra-relativistic heavy ion collisions, Phys. Rev. C 82 (2010) 044904, arXiv:1004.0805 [nucl-th].
[61] K. Werner, I. Karpenko, M. Bleicher, T. Pierog, S. Porteboeuf-Houssais, Jets, bulk matter, and their interaction in heavy ion collisions at several TeV, Phys. Rev. C 85 (2012) 064907, arXiv:1203.5704 [nucl-th].
[62] M. He, R.J. Fries, R. Rapp, Heavy flavor at the large hadron collider in a strong coupling approach, Phys. Lett. B 735 (2014) 445–450, arXiv:1401.3817 [nucl-th].
[63] J. Uphoff, O. Fochler, Z. Xu, C. Greiner, Elliptic flow and energy loss of heavy quarks in ultra-relativistic heavy ion collisions, Phys. Rev. C 84 (2011) 024908, arXiv:1104.2295 [hep-ph].
[64] O. Fochler, J. Uphoff, Z. Xu, C. Greiner, Jet quenching and elliptic flow at RHIC and LHC within a pQCD-based partonic transport model, J. Phys. G 38 (2011) 124152, arXiv:1107.0130 [hep-ph].
[65] J. Uphoff, O. Fochler, Z. Xu, C. Greiner, Open heavy flavor in Pb + Pb collisions at $\sqrt{s_{NN}} = 2.76$ TeV within a transport model, Phys. Lett. B 717 (2012) 430–435, arXiv:1205.4945 [hep-ph].

ALICE Collaboration

J. Adam [40], D. Adamová [83], M.M. Aggarwal [87], G. Aglieri Rinella [36], M. Agnello [110], N. Agrawal [48], Z. Ahammed [131], S.U. Ahn [68], S. Aiola [135], A. Akindinov [58], S.N. Alam [131], D. Aleksandrov [99], B. Alessandro [110], D. Alexandre [101], R. Alfaro Molina [64], A. Alici [104,12], A. Alkin [3], J.R.M. Almaraz [118], J. Alme [38], T. Alt [43], S. Altinpinar [18], I. Altsybeev [130], C. Alves Garcia Prado [119], C. Andrei [78], A. Andronic [96], V. Anguelov [93], J. Anielski [54], T. Antičić [97], F. Antinori [107], P. Antonioli [104], L. Aphecetche [112], H. Appelshäuser [53], S. Arcelli [28], N. Armesto [17], R. Arnaldi [110], I.C. Arsene [22], M. Arslandok [53], B. Audurier [112], A. Augustinus [36], R. Averbeck [96], M.D. Azmi [19], M. Bach [43], A. Badalà [106], Y.W. Baek [44], S. Bagnasco [110], R. Bailhache [53], R. Bala [90], A. Baldisseri [15], F. Baltasar Dos Santos Pedrosa [36], R.C. Baral [61], A.M. Barbano [110], R. Barbera [29], F. Barile [33], G.G. Barnaföldi [134], L.S. Barnby [101], V. Barret [70], P. Bartalini [7], K. Barth [36], J. Bartke [116], E. Bartsch [53], M. Basile [28], N. Bastid [70], S. Basu [131], B. Bathen [54], G. Batigne [112], A. Batista Camejo [70], B. Batyunya [66], P.C. Batzing [22], I.G. Bearden [80], H. Beck [53], C. Bedda [110], N.K. Behera [49,48], I. Belikov [55], F. Bellini [28], H. Bello Martinez [2], R. Bellwied [121], R. Belmont [133], E. Belmont-Moreno [64], V. Belyaev [76], G. Bencedi [134], S. Beole [27], I. Berceanu [78], A. Bercuci [78], Y. Berdnikov [85], D. Berenyi [134], R.A. Bertens [57], D. Berzano [27,36], L. Betev [36], A. Bhasin [90], I.R. Bhat [90], A.K. Bhati [87], B. Bhattacharjee [45], J. Bhom [127], L. Bianchi [121], N. Bianchi [72], C. Bianchin [133,57], J. Bielčík [40], J. Bielčíková [83], A. Bilandzic [80], R. Biswas [4], S. Biswas [79], S. Bjelogrlic [57], J.T. Blair [117], F. Blanco [10], D. Blau [99], C. Blume [53], F. Bock [93,74], A. Bogdanov [76], H. Bøggild [80], L. Boldizsár [134], M. Bombara [41], J. Book [53], H. Borel [15], A. Borissov [95], M. Borri [82], F. Bossú [65], E. Botta [27], S. Böttger [52], P. Braun-Munzinger [96], M. Bregant [119], T. Breitner [52], T.A. Broker [53], T.A. Browning [94], M. Broz [40], E.J. Brucken [46], E. Bruna [110], G.E. Bruno [33], D. Budnikov [98], H. Buesching [53], S. Bufalino [27,36], P. Buncic [36], O. Busch [127,93], Z. Buthelezi [65], J.B. Butt [16], J.T. Buxton [20], D. Caffarri [36], X. Cai [7], H. Caines [135], L. Calero Diaz [72], A. Caliva [57], E. Calvo Villar [102], P. Camerini [26], F. Carena [36], W. Carena [36], F. Carnesecchi [28], J. Castillo Castellanos [15], A.J. Castro [124], E.A.R. Casula [25], C. Cavicchioli [36], C. Ceballos Sanchez [9], J. Cepila [40], P. Cerello [110], J. Cerkala [114], B. Chang [122], S. Chapeland [36], M. Chartier [123], J.L. Charvet [15], S. Chattopadhyay [131], S. Chattopadhyay [100], V. Chelnokov [3], M. Cherney [86], C. Cheshkov [129], B. Cheynis [129], V. Chibante Barroso [36], D.D. Chinellato [120], P. Chochula [36], K. Choi [95], M. Chojnacki [80], S. Choudhury [131], P. Christakoglou [81], C.H. Christensen [80], P. Christiansen [34], T. Chujo [127], S.U. Chung [95], Z. Chunhui [57], C. Cicalo [105], L. Cifarelli [12,28], F. Cindolo [104], J. Cleymans [89], F. Colamaria [33], D. Colella [36,33,59], A. Collu [25], M. Colocci [28], G. Conesa Balbastre [71], Z. Conesa del Valle [51], M.E. Connors [135], J.G. Contreras [11,40], T.M. Cormier [84], Y. Corrales Morales [27], I. Cortés Maldonado [2], P. Cortese [32], M.R. Cosentino [119], F. Costa [36], P. Crochet [70], R. Cruz Albino [11], E. Cuautle [63], L. Cunqueiro [36], T. Dahms [92,37], A. Dainese [107], A. Danu [62], D. Das [100], I. Das [100,51], S. Das [4], A. Dash [120], S. Dash [48],

S. De [119], A. De Caro [31,12], G. de Cataldo [103], J. de Cuveland [43], A. De Falco [25], D. De Gruttola [12,31], N. De Marco [110], S. De Pasquale [31], A. Deisting [96,93], A. Deloff [77], E. Dénes [134,i], G. D'Erasmo [33], D. Di Bari [33], A. Di Mauro [36], P. Di Nezza [72], M.A. Diaz Corchero [10], T. Dietel [89], P. Dillenseger [53], R. Divià [36], Ø. Djuvsland [18], A. Dobrin [57,81], T. Dobrowolski [77,i], D. Domenicis Gimenez [119], B. Dönigus [53], O. Dordic [22], T. Drozhzhova [53], A.K. Dubey [131], A. Dubla [57], L. Ducroux [129], P. Dupieux [70], R.J. Ehlers [135], D. Elia [103], H. Engel [52], E. Epple [135], B. Erazmus [112,36], I. Erdemir [53], F. Erhardt [128], B. Espagnon [51], M. Estienne [112], S. Esumi [127], J. Eum [95], D. Evans [101], S. Evdokimov [111], G. Eyyubova [40], L. Fabbietti [37,92], D. Fabris [107], J. Faivre [71], A. Fantoni [72], M. Fasel [74], L. Feldkamp [54], D. Felea [62], A. Feliciello [110], G. Feofilov [130], J. Ferencei [83], A. Fernández Téllez [2], E.G. Ferreiro [17], A. Ferretti [27], A. Festanti [30], V.J.G. Feuillard [15,70], J. Figiel [116], M.A.S. Figueredo [123,119], S. Filchagin [98], D. Finogeev [56], F.M. Fionda [25], E.M. Fiore [33], M.G. Fleck [93], M. Floris [36], S. Foertsch [65], P. Foka [96], S. Fokin [99], E. Fragiacomo [109], A. Francescon [36,30], U. Frankenfeld [96], U. Fuchs [36], C. Furget [71], A. Furs [56], M. Fusco Girard [31], J.J. Gaardhøje [80], M. Gagliardi [27], A.M. Gago [102], M. Gallio [27], D.R. Gangadharan [74], P. Ganoti [88], C. Gao [7], C. Garabatos [96], E. Garcia-Solis [13], C. Gargiulo [36], P. Gasik [92,37], M. Germain [112], A. Gheata [36], M. Gheata [62,36], P. Ghosh [131], S.K. Ghosh [4], P. Gianotti [72], P. Giubellino [36,110], P. Giubilato [30], E. Gladysz-Dziadus [116], P. Glässel [93], D.M. Goméz Coral [64], A. Gomez Ramirez [52], P. González-Zamora [10], S. Gorbunov [43], L. Görlich [116], S. Gotovac [115], V. Grabski [64], L.K. Graczykowski [132], K.L. Graham [101], A. Grelli [57], A. Grigoras [36], C. Grigoras [36], V. Grigoriev [76], A. Grigoryan [1], S. Grigoryan [66], B. Grinyov [3], N. Grion [109], J.F. Grosse-Oetringhaus [36], J.-Y. Grossiord [129], R. Grosso [36], F. Guber [56], R. Guernane [71], B. Guerzoni [28], K. Gulbrandsen [80], H. Gulkanyan [1], T. Gunji [126], A. Gupta [90], R. Gupta [90], R. Haake [54], Ø. Haaland [18], C. Hadjidakis [51], M. Haiduc [62], H. Hamagaki [126], G. Hamar [134], J.W. Harris [135], A. Harton [13], D. Hatzifotiadou [104], S. Hayashi [126], S.T. Heckel [53], M. Heide [54], H. Helstrup [38], A. Herghelegiu [78], G. Herrera Corral [11], B.A. Hess [35], K.F. Hetland [38], T.E. Hilden [46], H. Hillemanns [36], B. Hippolyte [55], R. Hosokawa [127], P. Hristov [36], M. Huang [18], T.J. Humanic [20], N. Hussain [45], T. Hussain [19], D. Hutter [43], D.S. Hwang [21], R. Ilkaev [98], I. Ilkiv [77], M. Inaba [127], M. Ippolitov [76,99], M. Irfan [19], M. Ivanov [96], V. Ivanov [85], V. Izucheev [111], P.M. Jacobs [74], S. Jadlovska [114], C. Jahnke [119], H.J. Jang [68], M.A. Janik [132], P.H.S.Y. Jayarathna [121], C. Jena [30], S. Jena [121], R.T. Jimenez Bustamante [96], P.G. Jones [101], H. Jung [44], A. Jusko [101], P. Kalinak [59], A. Kalweit [36], J. Kamin [53], J.H. Kang [136], V. Kaplin [76], S. Kar [131], A. Karasu Uysal [69], O. Karavichev [56], T. Karavicheva [56], L. Karayan [93,96], E. Karpechev [56], U. Kebschull [52], R. Keidel [137], D.L.D. Keijdener [57], M. Keil [36], M. Mohisin Khan [19], P. Khan [100], S.A. Khan [131], A. Khanzadeev [85], Y. Kharlov [111], B. Kileng [38], B. Kim [136], D.W. Kim [44], D.J. Kim [122], H. Kim [136], J.S. Kim [44], M. Kim [44], M. Kim [136], S. Kim [21], T. Kim [136], S. Kirsch [43], I. Kisel [43], S. Kiselev [58], A. Kisiel [132], G. Kiss [134], J.L. Klay [6], C. Klein [53], J. Klein [93,36], C. Klein-Bösing [54], A. Kluge [36], M.L. Knichel [93], A.G. Knospe [117], T. Kobayashi [127], C. Kobdaj [113], M. Kofarago [36], T. Kollegger [43,96], A. Kolojvari [130], V. Kondratiev [130], N. Kondratyeva [76], E. Kondratyuk [111], A. Konevskikh [56], M. Kopcik [114], M. Kour [90], C. Kouzinopoulos [36], O. Kovalenko [77], V. Kovalenko [130], M. Kowalski [116], G. Koyithatta Meethaleveedu [48], J. Kral [122], I. Králik [59], A. Kravčáková [41], M. Kretz [43], M. Krivda [59,101], F. Krizek [83], E. Kryshen [36], M. Krzewicki [43], A.M. Kubera [20], V. Kučera [83], T. Kugathasan [36], C. Kuhn [55], P.G. Kuijer [81], A. Kumar [90], J. Kumar [48], L. Kumar [79,87], P. Kurashvili [77], A. Kurepin [56], A.B. Kurepin [56], A. Kuryakin [98], S. Kushpil [83], M.J. Kweon [50], Y. Kwon [136], S.L. La Pointe [110], P. La Rocca [29], C. Lagana Fernandes [119], I. Lakomov [36], R. Langoy [42], C. Lara [52], A. Lardeux [15], A. Lattuca [27], E. Laudi [36], R. Lea [26], L. Leardini [93], G.R. Lee [101], S. Lee [136], I. Legrand [36], F. Lehas [81], R.C. Lemmon [82], V. Lenti [103], E. Leogrande [57], I. León Monzón [118], M. Leoncino [27], P. Lévai [134], S. Li [7,70], X. Li [14], J. Lien [42], R. Lietava [101], S. Lindal [22], V. Lindenstruth [43], C. Lippmann [96], M.A. Lisa [20], H.M. Ljunggren [34], D.F. Lodato [57], P.I. Loenne [18], V. Loginov [76], C. Loizides [74], X. Lopez [70], E. López Torres [9], A. Lowe [134], P. Luettig [53], M. Lunardon [30], G. Luparello [26], P.H.F.N.D. Luz [119], A. Maevskaya [56], M. Mager [36], S. Mahajan [90], S.M. Mahmood [22], A. Maire [55], R.D. Majka [135], M. Malaev [85], I. Maldonado Cervantes [63], L. Malinina [66,ii], D. Mal'Kevich [58], P. Malzacher [96], A. Mamonov [98], V. Manko [99], F. Manso [70], V. Manzari [103,36], M. Marchisone [27], J. Mareš [60], G.V. Margagliotti [26], A. Margotti [104], J. Margutti [57], A. Marín [96], C. Markert [117], M. Marquard [53], N.A. Martin [96], J. Martin Blanco [112], P. Martinengo [36], M.I. Martínez [2], G. Martínez García [112], M. Martinez Pedreira [36], Y. Martynov [3], A. Mas [119], S. Masciocchi [96], M. Masera [27], A. Masoni [105], L. Massacrier [112], A. Mastroserio [33], H. Masui [127], A. Matyja [116], C. Mayer [116], J. Mazer [124], M.A. Mazzoni [108], D. Mcdonald [121], F. Meddi [24], Y. Melikyan [76],

A. Menchaca-Rocha [64], E. Meninno [31], J. Mercado Pérez [93], M. Meres [39], Y. Miake [127], M.M. Mieskolainen [46], K. Mikhaylov [66,58], L. Milano [36], J. Milosevic [22], L.M. Minervini [103,23], A. Mischke [57], A.N. Mishra [49], D. Miśkowiec [96], J. Mitra [131], C.M. Mitu [62], N. Mohammadi [57], B. Mohanty [131,79], L. Molnar [55], L. Montaño Zetina [11], E. Montes [10], M. Morando [30], D.A. Moreira De Godoy [112,54], L.A.P. Moreno [2], S. Moretto [30], A. Morreale [112], A. Morsch [36], V. Muccifora [72], E. Mudnic [115], D. Mühlheim [54], S. Muhuri [131], M. Mukherjee [131], J.D. Mulligan [135], M.G. Munhoz [119], R.H. Munzer [92,37], S. Murray [65], L. Musa [36], J. Musinsky [59], B.K. Nandi [48], R. Nania [104], E. Nappi [103], M.U. Naru [16], C. Nattrass [124], K. Nayak [79], T.K. Nayak [131], S. Nazarenko [98], A. Nedosekin [58], L. Nellen [63], F. Ng [121], M. Nicassio [96], M. Niculescu [62,36], J. Niedziela [36], B.S. Nielsen [80], S. Nikolaev [99], S. Nikulin [99], V. Nikulin [85], F. Noferini [104,12], P. Nomokonov [66], G. Nooren [57], J.C.C. Noris [2], J. Norman [123], A. Nyanin [99], J. Nystrand [18], H. Oeschler [93], S. Oh [135], S.K. Oh [67], A. Ohlson [36], A. Okatan [69], T. Okubo [47], L. Olah [134], J. Oleniacz [132], A.C. Oliveira Da Silva [119], M.H. Oliver [135], J. Onderwaater [96], C. Oppedisano [110], R. Orava [46], A. Ortiz Velasquez [63], A. Oskarsson [34], J. Otwinowski [116], K. Oyama [93], M. Ozdemir [53], Y. Pachmayer [93], P. Pagano [31], G. Paić [63], C. Pajares [17], S.K. Pal [131], J. Pan [133], A.K. Pandey [48], D. Pant [48], P. Papcun [114], V. Papikyan [1], G.S. Pappalardo [106], P. Pareek [49], W.J. Park [96], S. Parmar [87], A. Passfeld [54], V. Paticchio [103], R.N. Patra [131], B. Paul [100], T. Peitzmann [57], H. Pereira Da Costa [15], E. Pereira De Oliveira Filho [119], D. Peresunko [99,76], C.E. Pérez Lara [81], E. Perez Lezama [53], V. Peskov [53], Y. Pestov [5], V. Petráček [40], V. Petrov [111], M. Petrovici [78], C. Petta [29], S. Piano [109], M. Pikna [39], P. Pillot [112], O. Pinazza [104,36], L. Pinsky [121], D.B. Piyarathna [121], M. Płoskoń [74], M. Planinic [128], J. Pluta [132], S. Pochybova [134], P.L.M. Podesta-Lerma [118], M.G. Poghosyan [86,84], B. Polichtchouk [111], N. Poljak [128], W. Poonsawat [113], A. Pop [78], S. Porteboeuf-Houssais [70], J. Porter [74], J. Pospisil [83], S.K. Prasad [4], R. Preghenella [36,104], F. Prino [110], C.A. Pruneau [133], I. Pshenichnov [56], M. Puccio [110], G. Puddu [25], P. Pujahari [133], V. Punin [98], J. Putschke [133], H. Qvigstad [22], A. Rachevski [109], S. Raha [4], S. Rajput [90], J. Rak [122], A. Rakotozafindrabe [15], L. Ramello [32], F. Rami [55], R. Raniwala [91], S. Raniwala [91], S.S. Räsänen [46], B.T. Rascanu [53], D. Rathee [87], K.F. Read [124], J.S. Real [71], K. Redlich [77], R.J. Reed [133], A. Rehman [18], P. Reichelt [53], F. Reidt [93,36], X. Ren [7], R. Renfordt [53], A.R. Reolon [72], A. Reshetin [56], F. Rettig [43], J.-P. Revol [12], K. Reygers [93], V. Riabov [85], R.A. Ricci [73], T. Richert [34], M. Richter [22], P. Riedler [36], W. Riegler [36], F. Riggi [29], C. Ristea [62], A. Rivetti [110], E. Rocco [57], M. Rodríguez Cahuantzi [2], A. Rodriguez Manso [81], K. Røed [22], E. Rogochaya [66], D. Rohr [43], D. Röhrich [18], R. Romita [123], F. Ronchetti [72,36], L. Ronflette [112], P. Rosnet [70], A. Rossi [30,36], F. Roukoutakis [88], A. Roy [49], C. Roy [55], P. Roy [100], A.J. Rubio Montero [10], R. Rui [26], R. Russo [27], E. Ryabinkin [99], Y. Ryabov [85], A. Rybicki [116], S. Sadovsky [111], K. Šafařík [36], B. Sahlmuller [53], P. Sahoo [49], R. Sahoo [49], S. Sahoo [61], P.K. Sahu [61], J. Saini [131], S. Sakai [72], M.A. Saleh [133], C.A. Salgado [17], J. Salzwedel [20], S. Sambyal [90], V. Samsonov [85], L. Šándor [59], A. Sandoval [64], M. Sano [127], D. Sarkar [131], E. Scapparone [104], F. Scarlassara [30], R.P. Scharenberg [94], C. Schiaua [78], R. Schicker [93], C. Schmidt [96], H.R. Schmidt [35], S. Schuchmann [53], J. Schukraft [36], M. Schulc [40], T. Schuster [135], Y. Schutz [112,36], K. Schwarz [96], K. Schweda [96], G. Scioli [28], E. Scomparin [110], R. Scott [124], J.E. Seger [86], Y. Sekiguchi [126], D. Sekihata [47], I. Selyuzhenkov [96], K. Senosi [65], J. Seo [95,67], E. Serradilla [64,10], A. Sevcenco [62], A. Shabanov [56], A. Shabetai [112], O. Shadura [3], R. Shahoyan [36], A. Shangaraev [111], A. Sharma [90], M. Sharma [90], M. Sharma [90], N. Sharma [124,61], K. Shigaki [47], K. Shtejer [9,27], Y. Sibiriak [99], S. Siddhanta [105], K.M. Sielewicz [36], T. Siemiarczuk [77], D. Silvermyr [84,34], C. Silvestre [71], G. Simatovic [128], G. Simonetti [36], R. Singaraju [131], R. Singh [79], S. Singha [131,79], V. Singhal [131], B.C. Sinha [131], T. Sinha [100], B. Sitar [39], M. Sitta [32], T.B. Skaali [22], M. Slupecki [122], N. Smirnov [135], R.J.M. Snellings [57], T.W. Snellman [122], C. Søgaard [34], R. Soltz [75], J. Song [95], M. Song [136], Z. Song [7], F. Soramel [30], S. Sorensen [124], M. Spacek [40], E. Spiriti [72], I. Sputowska [116], M. Spyropoulou-Stassinaki [88], B.K. Srivastava [94], J. Stachel [93], I. Stan [62], G. Stefanek [77], E. Stenlund [34], G. Steyn [65], J.H. Stiller [93], D. Stocco [112], P. Strmen [39], A.A.P. Suaide [119], T. Sugitate [47], C. Suire [51], M. Suleymanov [16], M. Suljic [26,i], R. Sultanov [58], M. Šumbera [83], T.J.M. Symons [74], A. Szabo [39], A. Szanto de Toledo [119,i], I. Szarka [39], A. Szczepankiewicz [36], M. Szymanski [132], U. Tabassam [16], J. Takahashi [120], G.J. Tambave [18], N. Tanaka [127], M.A. Tangaro [33], J.D. Tapia Takaki [51,iii], A. Tarantola Peloni [53], M. Tarhini [51], M. Tariq [19], M.G. Tarzila [78], A. Tauro [36], G. Tejeda Muñoz [2], A. Telesca [36], K. Terasaki [126], C. Terrevoli [30,25], B. Teyssier [129], J. Thäder [74,96], D. Thomas [117], R. Tieulent [129], A.R. Timmins [121], A. Toia [53], S. Trogolo [110], V. Trubnikov [3], W.H. Trzaska [122], T. Tsuji [126], A. Tumkin [98], R. Turrisi [107], T.S. Tveter [22], K. Ullaland [18], A. Uras [129], G.L. Usai [25], A. Utrobicic [128],

M. Vajzer [83], L. Valencia Palomo [70], S. Vallero [27], J. Van Der Maarel [57], J.W. Van Hoorne [36], M. van Leeuwen [57], T. Vanat [83], P. Vande Vyvre [36], D. Varga [134], A. Vargas [2], M. Vargyas [122], R. Varma [48], M. Vasileiou [88], A. Vasiliev [99], A. Vauthier [71], V. Vechernin [130], A.M. Veen [57], M. Veldhoen [57], A. Velure [18], M. Venaruzzo [73], E. Vercellin [27], S. Vergara Limón [2], R. Vernet [8], M. Verweij [133,36], L. Vickovic [115], G. Viesti [30,i], J. Viinikainen [122], Z. Vilakazi [125], O. Villalobos Baillie [101], A. Villatoro Tello [2], A. Vinogradov [99], L. Vinogradov [130], Y. Vinogradov [98,i], T. Virgili [31], V. Vislavicius [34], Y.P. Viyogi [131], A. Vodopyanov [66], M.A. Völkl [93], K. Voloshin [58], S.A. Voloshin [133], G. Volpe [134,36], B. von Haller [36], I. Vorobyev [92,37], D. Vranic [96,36], J. Vrláková [41], B. Vulpescu [70], A. Vyushin [98], B. Wagner [18], J. Wagner [96], H. Wang [57], M. Wang [7,112], D. Watanabe [127], Y. Watanabe [126], M. Weber [36], S.G. Weber [96], J.P. Wessels [54], U. Westerhoff [54], J. Wiechula [35], J. Wikne [22], M. Wilde [54], G. Wilk [77], J. Wilkinson [93], M.C.S. Williams [104], B. Windelband [93], M. Winn [93], C.G. Yaldo [133], H. Yang [57], P. Yang [7], S. Yano [47], Z. Yin [7], H. Yokoyama [127], I.-K. Yoo [95], V. Yurchenko [3], I. Yushmanov [99], A. Zaborowska [132], V. Zaccolo [80], A. Zaman [16], C. Zampolli [104], H.J.C. Zanoli [119], S. Zaporozhets [66], N. Zardoshti [101], A. Zarochentsev [130], P. Závada [60], N. Zaviyalov [98], H. Zbroszczyk [132], I.S. Zgura [62], M. Zhalov [85], H. Zhang [18,7], X. Zhang [74,7], Y. Zhang [7], Z. Zhang [7], C. Zhao [22], N. Zhigareva [58], D. Zhou [7], Y. Zhou [80,57], Z. Zhou [18], H. Zhu [18,7], J. Zhu [7,112], A. Zichichi [28,12], A. Zimmermann [93], M.B. Zimmermann [36,54], G. Zinovjev [3], M. Zyzak [43]

[1] *A.I. Alikhanyan National Science Laboratory (Yerevan Physics Institute) Foundation, Yerevan, Armenia*
[2] *Benemérita Universidad Autónoma de Puebla, Puebla, Mexico*
[3] *Bogolyubov Institute for Theoretical Physics, Kiev, Ukraine*
[4] *Bose Institute, Department of Physics and Centre for Astroparticle Physics and Space Science (CAPSS), Kolkata, India*
[5] *Budker Institute for Nuclear Physics, Novosibirsk, Russia*
[6] *California Polytechnic State University, San Luis Obispo, CA, United States*
[7] *Central China Normal University, Wuhan, China*
[8] *Centre de Calcul de l'IN2P3, Villeurbanne, France*
[9] *Centro de Aplicaciones Tecnológicas y Desarrollo Nuclear (CEADEN), Havana, Cuba*
[10] *Centro de Investigaciones Energéticas Medioambientales y Tecnológicas (CIEMAT), Madrid, Spain*
[11] *Centro de Investigación y de Estudios Avanzados (CINVESTAV), Mexico City and Mérida, Mexico*
[12] *Centro Fermi – Museo Storico della Fisica e Centro Studi e Ricerche "Enrico Fermi", Rome, Italy*
[13] *Chicago State University, Chicago, IL, USA*
[14] *China Institute of Atomic Energy, Beijing, China*
[15] *Commissariat à l'Energie Atomique, IRFU, Saclay, France*
[16] *COMSATS Institute of Information Technology (CIIT), Islamabad, Pakistan*
[17] *Departamento de Física de Partículas and IGFAE, Universidad de Santiago de Compostela, Santiago de Compostela, Spain*
[18] *Department of Physics and Technology, University of Bergen, Bergen, Norway*
[19] *Department of Physics, Aligarh Muslim University, Aligarh, India*
[20] *Department of Physics, Ohio State University, Columbus, OH, United States*
[21] *Department of Physics, Sejong University, Seoul, South Korea*
[22] *Department of Physics, University of Oslo, Oslo, Norway*
[23] *Dipartimento di Elettrotecnica ed Elettronica del Politecnico, Bari, Italy*
[24] *Dipartimento di Fisica dell'Università 'La Sapienza' and Sezione INFN, Rome, Italy*
[25] *Dipartimento di Fisica dell'Università and Sezione INFN, Cagliari, Italy*
[26] *Dipartimento di Fisica dell'Università and Sezione INFN, Trieste, Italy*
[27] *Dipartimento di Fisica dell'Università and Sezione INFN, Turin, Italy*
[28] *Dipartimento di Fisica e Astronomia dell'Università and Sezione INFN, Bologna, Italy*
[29] *Dipartimento di Fisica e Astronomia dell'Università and Sezione INFN, Catania, Italy*
[30] *Dipartimento di Fisica e Astronomia dell'Università and Sezione INFN, Padova, Italy*
[31] *Dipartimento di Fisica 'E.R. Caianiello' dell'Università and Gruppo Collegato INFN, Salerno, Italy*
[32] *Dipartimento di Scienze e Innovazione Tecnologica dell'Università del Piemonte Orientale and Gruppo Collegato INFN, Alessandria, Italy*
[33] *Dipartimento Interateneo di Fisica 'M. Merlin' and Sezione INFN, Bari, Italy*
[34] *Division of Experimental High Energy Physics, University of Lund, Lund, Sweden*
[35] *Eberhard Karls Universität Tübingen, Tübingen, Germany*
[36] *European Organization for Nuclear Research (CERN), Geneva, Switzerland*
[37] *Excellence Cluster Universe, Technische Universität München, Munich, Germany*
[38] *Faculty of Engineering, Bergen University College, Bergen, Norway*
[39] *Faculty of Mathematics, Physics and Informatics, Comenius University, Bratislava, Slovakia*
[40] *Faculty of Nuclear Sciences and Physical Engineering, Czech Technical University in Prague, Prague, Czech Republic*
[41] *Faculty of Science, P.J. Šafárik University, Košice, Slovakia*
[42] *Faculty of Technology, Buskerud and Vestfold University College, Vestfold, Norway*
[43] *Frankfurt Institute for Advanced Studies, Johann Wolfgang Goethe-Universität Frankfurt, Frankfurt, Germany*
[44] *Gangneung-Wonju National University, Gangneung, South Korea*
[45] *Gauhati University, Department of Physics, Guwahati, India*
[46] *Helsinki Institute of Physics (HIP), Helsinki, Finland*
[47] *Hiroshima University, Hiroshima, Japan*
[48] *Indian Institute of Technology Bombay (IIT), Mumbai, India*
[49] *Indian Institute of Technology Indore, Indore (IITI), India*
[50] *Inha University, Incheon, South Korea*
[51] *Institut de Physique Nucléaire d'Orsay (IPNO), Université Paris-Sud, CNRS-IN2P3, Orsay, France*
[52] *Institut für Informatik, Johann Wolfgang Goethe-Universität Frankfurt, Frankfurt, Germany*
[53] *Institut für Kernphysik, Johann Wolfgang Goethe-Universität Frankfurt, Frankfurt, Germany*
[54] *Institut für Kernphysik, Westfälische Wilhelms-Universität Münster, Münster, Germany*

[55] Institut Pluridisciplinaire Hubert Curien (IPHC), Université de Strasbourg, CNRS-IN2P3, Strasbourg, France
[56] Institute for Nuclear Research, Academy of Sciences, Moscow, Russia
[57] Institute for Subatomic Physics of Utrecht University, Utrecht, Netherlands
[58] Institute for Theoretical and Experimental Physics, Moscow, Russia
[59] Institute of Experimental Physics, Slovak Academy of Sciences, Košice, Slovakia
[60] Institute of Physics, Academy of Sciences of the Czech Republic, Prague, Czech Republic
[61] Institute of Physics, Bhubaneswar, India
[62] Institute of Space Science (ISS), Bucharest, Romania
[63] Instituto de Ciencias Nucleares, Universidad Nacional Autónoma de México, Mexico City, Mexico
[64] Instituto de Física, Universidad Nacional Autónoma de México, Mexico City, Mexico
[65] iThemba LABS, National Research Foundation, Somerset West, South Africa
[66] Joint Institute for Nuclear Research (JINR), Dubna, Russia
[67] Konkuk University, Seoul, South Korea
[68] Korea Institute of Science and Technology Information, Daejeon, South Korea
[69] KTO Karatay University, Konya, Turkey
[70] Laboratoire de Physique Corpusculaire (LPC), Clermont Université, Université Blaise Pascal, CNRS-IN2P3, Clermont-Ferrand, France
[71] Laboratoire de Physique Subatomique et de Cosmologie, Université Grenoble-Alpes, CNRS-IN2P3, Grenoble, France
[72] Laboratori Nazionali di Frascati, INFN, Frascati, Italy
[73] Laboratori Nazionali di Legnaro, INFN, Legnaro, Italy
[74] Lawrence Berkeley National Laboratory, Berkeley, CA, United States
[75] Lawrence Livermore National Laboratory, Livermore, CA, United States
[76] Moscow Engineering Physics Institute, Moscow, Russia
[77] National Centre for Nuclear Studies, Warsaw, Poland
[78] National Institute for Physics and Nuclear Engineering, Bucharest, Romania
[79] National Institute of Science Education and Research, Bhubaneswar, India
[80] Niels Bohr Institute, University of Copenhagen, Copenhagen, Denmark
[81] Nikhef, Nationaal Instituut voor Subatomaire Fysica, Amsterdam, Netherlands
[82] Nuclear Physics Group, STFC Daresbury Laboratory, Daresbury, United Kingdom
[83] Nuclear Physics Institute, Academy of Sciences of the Czech Republic, Řež u Prahy, Czech Republic
[84] Oak Ridge National Laboratory, Oak Ridge, TN, United States
[85] Petersburg Nuclear Physics Institute, Gatchina, Russia
[86] Physics Department, Creighton University, Omaha, NE, United States
[87] Physics Department, Panjab University, Chandigarh, India
[88] Physics Department, University of Athens, Athens, Greece
[89] Physics Department, University of Cape Town, Cape Town, South Africa
[90] Physics Department, University of Jammu, Jammu, India
[91] Physics Department, University of Rajasthan, Jaipur, India
[92] Physik Department, Technische Universität München, Munich, Germany
[93] Physikalisches Institut, Ruprecht-Karls-Universität Heidelberg, Heidelberg, Germany
[94] Purdue University, West Lafayette, IN, United States
[95] Pusan National University, Pusan, South Korea
[96] Research Division and ExtreMe Matter Institute EMMI, GSI Helmholtzzentrum für Schwerionenforschung, Darmstadt, Germany
[97] Rudjer Bošković Institute, Zagreb, Croatia
[98] Russian Federal Nuclear Center (VNIIEF), Sarov, Russia
[99] Russian Research Centre Kurchatov Institute, Moscow, Russia
[100] Saha Institute of Nuclear Physics, Kolkata, India
[101] School of Physics and Astronomy, University of Birmingham, Birmingham, United Kingdom
[102] Sección Física, Departamento de Ciencias, Pontificia Universidad Católica del Perú, Lima, Peru
[103] Sezione INFN, Bari, Italy
[104] Sezione INFN, Bologna, Italy
[105] Sezione INFN, Cagliari, Italy
[106] Sezione INFN, Catania, Italy
[107] Sezione INFN, Padova, Italy
[108] Sezione INFN, Rome, Italy
[109] Sezione INFN, Trieste, Italy
[110] Sezione INFN, Turin, Italy
[111] SSC IHEP of NRC Kurchatov institute, Protvino, Russia
[112] SUBATECH, Ecole des Mines de Nantes, Université de Nantes, CNRS-IN2P3, Nantes, France
[113] Suranaree University of Technology, Nakhon Ratchasima, Thailand
[114] Technical University of Košice, Košice, Slovakia
[115] Technical University of Split FESB, Split, Croatia
[116] The Henryk Niewodniczanski Institute of Nuclear Physics, Polish Academy of Sciences, Cracow, Poland
[117] The University of Texas at Austin, Physics Department, Austin, TX, USA
[118] Universidad Autónoma de Sinaloa, Culiacán, Mexico
[119] Universidade de São Paulo (USP), São Paulo, Brazil
[120] Universidade Estadual de Campinas (UNICAMP), Campinas, Brazil
[121] University of Houston, Houston, TX, United States
[122] University of Jyväskylä, Jyväskylä, Finland
[123] University of Liverpool, Liverpool, United Kingdom
[124] University of Tennessee, Knoxville, TN, United States
[125] University of the Witwatersrand, Johannesburg, South Africa
[126] University of Tokyo, Tokyo, Japan
[127] University of Tsukuba, Tsukuba, Japan
[128] University of Zagreb, Zagreb, Croatia
[129] Université de Lyon, Université Lyon 1, CNRS/IN2P3, IPN-Lyon, Villeurbanne, France
[130] V. Fock Institute for Physics, St. Petersburg State University, St. Petersburg, Russia
[131] Variable Energy Cyclotron Centre, Kolkata, India
[132] Warsaw University of Technology, Warsaw, Poland
[133] Wayne State University, Detroit, MI, United States

[134] *Wigner Research Centre for Physics, Hungarian Academy of Sciences, Budapest, Hungary*
[135] *Yale University, New Haven, CT, United States*
[136] *Yonsei University, Seoul, South Korea*
[137] *Zentrum für Technologietransfer und Telekommunikation (ZTT), Fachhochschule Worms, Worms, Germany*

[i] Deceased.
[ii] Also at: M.V. Lomonosov Moscow State University, D.V. Skobeltsyn Institute of Nuclear, Physics, Moscow, Russia.
[iii] Also at: University of Kansas, Lawrence, Kansas, United States.